Global and Planetary Change 125 (2015) 13–35

Contents lists available at ScienceDirect

Global and Planetary Change

journal homepage: www.elsevier.com/locate/gloplacha

Invited review

Arctic freshwater export: Status, mechanisms, and prospects

Thomas W.N. Haine [a,*], Beth Curry [b], Rüdiger Gerdes [c], Edmond Hansen [d], Michael Karcher [c,e], Craig Lee [b], Bert Rudels [f], Gunnar Spreen [d], Laura de Steur [d,g], Kial D. Stewart [h], Rebecca Woodgate [b]

[a] Earth & Planetary Sciences, The Johns Hopkins University, Baltimore, MD, USA
[b] Applied Physics Laboratory, University of Washington, WA, USA
[c] Alfred Wegener Institute for Polar and Marine Research, Bremerhaven, Germany
[d] Norwegian Polar Institute, Fram Centre, Tromsø, Norway
[e] Ocean Atmosphere Systems GmbH, Hamburg, Germany
[f] Finnish Meteorological Institute, Helsinki, Finland
[g] NIOZ Royal Netherlands Institute for Sea Research, Den Burg, The Netherlands
[h] Climate Change Research Centre, University of New South Wales, Sydney, Australia

ARTICLE INFO

Article history:
Received 22 July 2014
Received in revised form 17 November 2014
Accepted 26 November 2014
Available online 4 December 2014

Keywords:
Arctic Ocean
hydrological cycle
oceanography
climate change

ABSTRACT

Large freshwater anomalies clearly exist in the Arctic Ocean. For example, liquid freshwater has accumulated in the Beaufort Gyre in the decade of the 2000s compared to 1980–2000, with an extra ≈5000 km^3 — about 25% — being stored. The sources of freshwater to the Arctic from precipitation and runoff have increased between these periods (most of the evidence comes from models). Despite flux increases from 2001 to 2011, it is uncertain if the marine freshwater source through Bering Strait for the 2000s has changed, as observations in the 1980s and 1990s are incomplete. The marine freshwater fluxes draining the Arctic through Fram and Davis straits are also insignificantly different. In this way, the balance of sources and sinks of freshwater to the Arctic, Canadian Arctic Archipelago (CAA), and Baffin Bay shifted to about 1200 ± 730 km^3 yr^{-1} freshening the region, on average, during the 2000s. The observed accumulation of liquid freshwater is consistent with this increased supply and the loss of freshwater from sea ice. Coupled climate models project continued freshening of the Arctic during the 21st century, with a total gain of about 50,000 km^3 for the Arctic, CAA, and Baffin Bay (an increase of about 50%) by 2100. Understanding of the mechanisms controlling freshwater emphasizes the importance of Arctic surface winds, in addition to the sources of freshwater. The wind can modify the storage, release, and pathways of freshwater on timescales of O(1–10) months. Discharges of excess freshwater through Fram or Davis straits appear possible, triggered by changes in the wind, but are hard to predict. Continued measurement of the fluxes and storage of freshwater is needed to observe changes such as these.

Contents

* Corresponding author at: 329 Olin Hall, The Johns Hopkins University, 3400 N. Charles St., Baltimore, MD 21218, USA. Tel.: +1 410 516 7048.
E-mail address: Thomas.Haine@jhu.edu (T.W.N. Haine).

http://dx.doi.org/10.1016/j.gloplacha.2014.11.013
0921-8181/

1. Introduction

Large changes have been seen in the Arctic Ocean freshwater system in recent years, particularly as the observational database ballooned during the International Polar Year (2007–2008). Moreover, oceanographic measurements of freshwater leaving the Arctic through the Canadian Arctic Archipelago (CAA) and Nordic Seas now span a decade. With further widespread changes forecast, the time is ripe for a review and synthesis of knowledge on the freshwater system of the Arctic and Subarctic Ocean. That is our task here. We review current understanding on the status, mechanisms, and prospects for Arctic freshwater, focusing on freshwater export to the Atlantic Ocean. Where possible we synthesize this knowledge to draw new conclusions. The overall goal is to describe recent changes in the Arctic Ocean freshwater system, to attempt to understand the mechanisms causing these changes, and, on this basis, to speculate about future prospects, especially for the oceanic export of Arctic freshwater. In particular, we consider the budget of Arctic freshwater, quantifying the storage of freshwater, and the various sources and sinks (Section 2). In Section 3 understanding of the mechanisms controlling the Arctic freshwater budget is discussed. The prospects for changes in the budget and export fluxes in the coming years and decades are covered in Section 4.

Why is the Arctic freshwater system important for global planetary change? The principal reasons are these: First, the Arctic freshwater system is one terminus of the global atmospheric cycle that carries water from low to high latitudes. Evaporation from the warm tropics leads to condensation, precipitation, and accumulation over the cold poles. Second, freshwater plays a leading role in Arctic climate dynamics and climate change. Freshwater as ice reflects solar radiation because of its relatively high albedo; freshwater as liquid forms a thin boundary layer (the halocline) that separates the warmer water below from the atmosphere. Recent changes in the Arctic freshwater system, such as the large decrease of sea ice in summer, support the view that Arctic anthropogenic change is amplified with respect to the global average. Finally, the Arctic freshwater system impacts manifold physical and biological processes, both within the Arctic itself, and at lower latitudes. Many of these processes influence human activities.

Fig. 1 shows the region of interest. We consider freshwater, as both liquid and ice, in the Arctic Ocean, CAA, and Baffin Bay. This control volume is closed by oceanic sections at the Bering Strait (50 m deep, 85 km wide), the Fram Strait (2600 m deep, 580 km wide), the Davis Strait (1030 m deep, 330 km wide), and the Barents Sea Opening (480 m deep, 820 km wide). The fluxes of mass, heat, and freshwater have been monitored across these sections with oceanographic mooring arrays and ship-based surveys. The export of freshwater through Davis Strait captures the branch of the Arctic outflow through the CAA. The export through western Fram Strait is the other major export pathway, draining the central Arctic of liquid freshwater and sea ice. In the discussion of these fluxes, we emphasize low-frequency changes, contrasting the decade of the 2000s with the 1980s and 1990s. Seasonal and interannual variations are not discussed in detail.

This paper emerged from a meeting of the Arctic–Subarctic Ocean Flux program (http://asof.awi.de/) in autumn 2012, kindly hosted by the Istituto delle Scienze Marine, Lerici, Italy.

2. Status of freshwater storage and export

Freshwater in the Arctic Ocean exists in the solid form as sea ice (frozen seawater) and in the liquid form. Liquid freshwater dilutes the upper layers of the Arctic Ocean to create the ubiquitous halocline (the 10–50 m thick near-surface layer of strongly-increasing salinity with depth). Understanding Arctic freshwater involves quantifying where these two phases are stored, and how they are transported and redistributed. Quantifying storage requires knowledge of the distribution in space of liquid freshwater and sea ice.[1] Quantifying transport requires knowledge of the fluxes of freshwater into and out of the Arctic Ocean. Knowledge of freshwater storage and transport allows the construction of a freshwater budget. The goal in this section is to review the current knowledge of freshwater storage and fluxes and to update the freshwater budget for the Arctic Ocean. The two overarching

[1] Freshwater storage in the Arctic is quantified by the amount of zero-salinity water required to reach the observed salinity of a seawater sample starting from a particular reference salinity. In a similar way, transport of freshwater is quantified as the equivalent flux of zero salinity water. Specifically, liquid freshwater content m (in meters) is estimated as

$$m = \int_D^\eta \frac{S_{\mathrm{ref}} - S}{S_{\mathrm{ref}}} \mathrm{d}z \tag{1}$$

for salinity S (all salinities are on the practical salinity scale). The reference salinity S_{ref} equals 34.80, following Aagaard and Carmack (1989) and Serreze et al. (2006), unless otherwise stated. It is close to the mean salinity for the region of interest (Tsubouchi et al., 2012). The integration with depth z is performed over the fresh upper levels between the S_{ref} isohaline surface, whose depth is D, and the sea surface at height η. Occasionally, D is taken as the depth of a different isohaline surface (for example, Rabe et al. (2011) take $S_{\mathrm{ref}} = 35$, but D is the depth of the 34 isohaline). Integrating m over horizontal area yields the total liquid freshwater content (a volume, or inventory, that we quote in km^3).

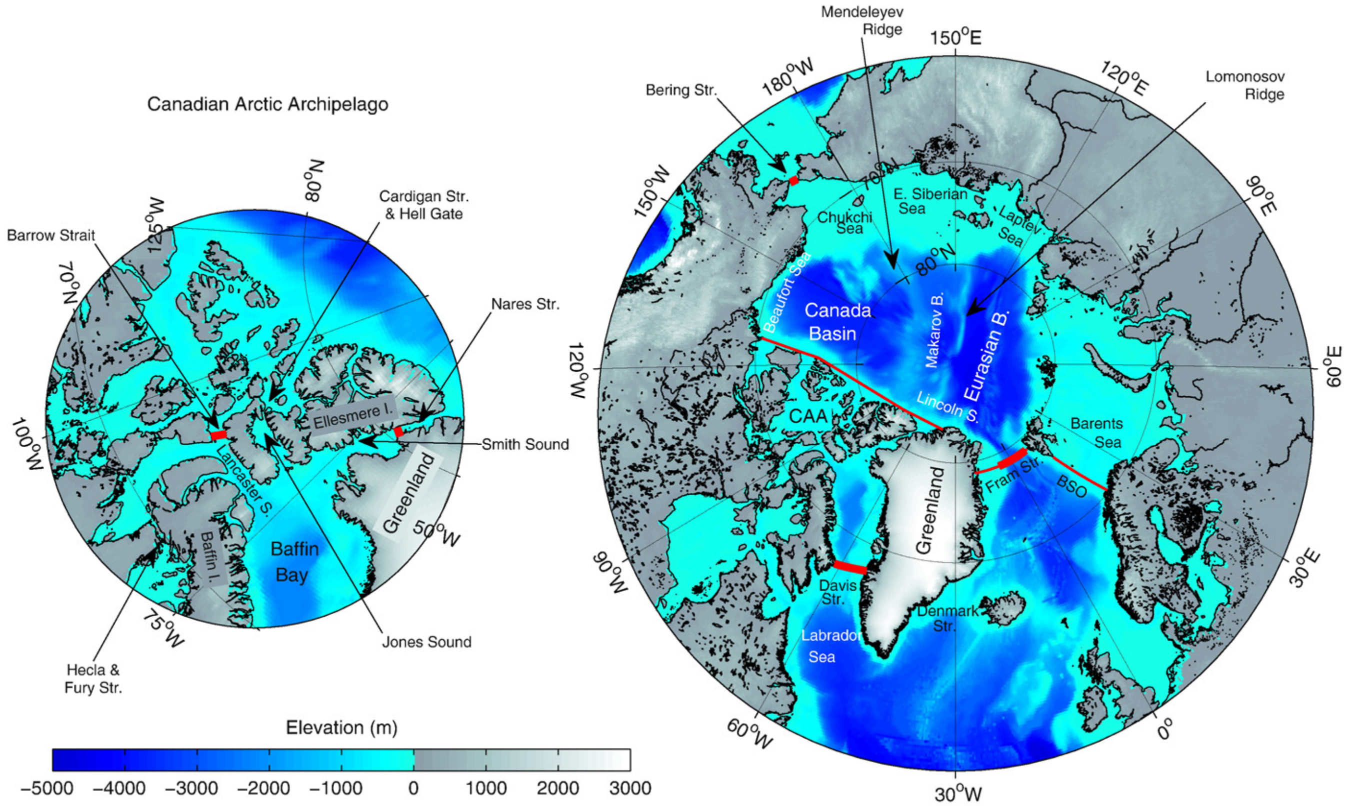

Fig. 1. Map of the Arctic and subpolar North Atlantic oceans and the Canadian Arctic Archipelago (CAA). The main oceanic flux monitoring sites are indicated with thick red lines. Thin red lines in the main map are used to delimit the Arctic Ocean (and the boundaries of Serreze et al.'s (2006) domain; see Section 2.1). The freshwater budget discussed in Section 2 considers the Arctic, CAA, and Baffin Bay contained within the Bering, Davis and Fram straits, and the Barents Sea Opening (BSO). The bathymetry (topography; from Terrainbase (1995)) is shown with blue (gray) colors in meters above sea level.

questions are: What is the current state of freshwater storage in the Arctic Ocean/CAA and freshwater exchange with neighboring reservoirs? And, where are the greatest uncertainties in freshwater storage and export given the present and anticipated observing efforts? A summary and a graphical view of the past, present and anticipated future freshwater budget of the Arctic Ocean are provided in Table 1 and Fig. 2. The left hand panel of Fig. 2 shows the budget for, nominally, 1980–2000, the period we initially consider. The right panel shows the budget for the 2000s (Sections 2.2, 2.3, 2.4).

2.1. Pre-2000 freshwater budget

Aagaard and Carmack (1989) provided the first modern account of the complete freshwater budget of the Arctic Ocean. Budget estimates change over time, however, for two reasons: First, new data are collected and the historical databases grow and, second, the system itself changes. For these reasons, this pioneering overview was updated by Lewis et al. (2000), Peterson et al. (2006), Serreze et al. (2006), White et al. (2007), Dickson et al. (2007, 2008), Rawlins et al. (2010) and Beszczynska-Möller et al. (2011). These assessments synthesized information from individually-published studies on the different components of the Arctic freshwater system. For example, Serreze et al. (2006) used the long-term Polar Science Center Hydrographic Climatology (PHC, version 3.0, updated from Steele et al. (2001)) to estimate the total annual-mean liquid freshwater content of the Arctic Ocean to be 74,000 km^3 (see also Serreze et al. (2008)). This volume includes all basins and the surrounding shelves in a domain defined by lines across the Fram Strait, the Barents Sea Opening, the Bering Strait, and the northern entrance to the CAA (see Fig. 1). Freshwater storage is distributed unevenly; more than half resides in the Canadian Basin, with about 25% in the Beaufort Gyre.[2] The CAA (as far as Hecla and Fury straits) and Baffin Bay (as far as Davis Strait) store about 19,000 km^3 extra freshwater based on the PHC 3.0 climatology for a total of around 93,000 km^3 (Table 1, Fig. 2).

Freshwater storage as solid sea ice is the component of the Arctic freshwater budget with most uncertainty. Horizontal sea ice extent is relatively well known from direct satellite observations, at least since 1979. The uncertainty in sea ice volume is due to sparse information on the spatial and seasonal distributions of Arctic ice thickness. In constructing their sea ice budget, Aagaard and Carmack (1989) assumed a value of 3 m for the mean sea ice thickness.[3] This number multiplied by the 1973–1976 satellite-derived ice coverage yields a freshwater volume stored in sea ice of 17,300 km^3 (in the annual average, and consistent with the 1980–2000 average of 17,800 km^3, quoted below in Section 2.3).[4] Serreze et al. (2006) followed the same approach; they chose a mean ice thickness of 2 m, reflecting the general thinning taking place across the Arctic. Multiplied with the 1979–2001 satellite-derived mean sea-ice coverage, Serreze et al. (2006) estimated that about

[2] The Beaufort Gyre circulates above the deep Canada Basin (see Fig. 5 below). The Canadian Basin includes the Canada and Makarov basins. The Beaufort Sea includes the shelf and slope regions north of Alaska and northwest Canada (Fig. 1).

[3] Kwok and Rothrock (2009) report mean ice thickness from submarine data for the Central Arctic at the end of the melt season of 3.02 m for 1958–1976. Laxon et al. (2003) report a mean winter (October to March) ice thickness of 2.73 m for 1993–2001 from radar altimetry south of 82°N.

[4] Sea ice typically has an average salinity, S_{ice}, of about 4 (Aagaard and Carmack 1989; it decreases with age). For ease of comparison, we quote the equivalent liquid freshwater volume stored in sea ice throughout. Namely, we multiply ice volume fluxes by $(1 - S_{ice}/S_{ref})(\rho_{ice}/\rho_w)$, where $\rho_{ice} = 900$ kg m^{-3} is the average density of ice, and $\rho_w = 1003$ kg m^{-3} is the density of seawater with salinity S_{ice}.

Table 1
Arctic/CAA freshwater reservoir volumes and fluxes computed with respect to a reference salinity of 34.80 (positive fluxes freshen the Arctic; see also Fig. 1).

	1980–2000[a]	2000–2010[b]	21st century[c]
Freshwater reservoirs (km^3)			
Liquid freshwater	93,000	101,000	150,000 by 2100 (Fig. 9)
Beaufort Gyre	18,500	23,500	Increases (with fluctuations?)
As seasonal sea ice[d]	13,000	13,400	Increases?
As multiyear sea ice[e]	10,900	7400	Decreases
As average sea ice	17,800	14,300	3000 by 2100
Total freshwater volume	110,800	115,300	~150,000 by 2100
Freshwater fluxes (km^3 yr^{-1})			
Runoff	3900 ± 390	4200 ± 420	5500 by 2100
Bering Strait (liquid)	2400? ± 300+[f]	2500 ± 100	>2500
Bering Strait (in sea ice)	140 ± 40	140 ± 40	?
P − E	2000 ± 200	2200 ± 220	2500 by 2100
Greenland flux	330 ± 20	370 ± 25	430 by 2025
Davis Strait (liquid)	−3200 ± 320	−2900 ± 190	−4000 by 2070; −3500 by 2100
Davis Strait (in sea ice)	−160 ± ?	−320 ± 45	?
Fram Strait (liquid)[g]	−2700 ± 530	−2800 ± 420	−6000 by 2100
Fram Strait (in sea ice)	−2300 ± 340	−1900 ± 280	−600 by 2100
Barents Sea Opening	−90 ± 90	−90 ± 90	?
Fury and Hecla straits	−200 ± ?	−200 ± ?	?
Total fluxes (km^3 yr^{-1})			
Inflow sources	8800 ± 530?	9400 ± 490	≳11,000 by 2100
Outflow sinks	−8700 ± 700	−8250 ± 550	−10,000 by 2100
Residual	100 ± 900?	1200 ± 730	~1000 by 2100?

[a] Taken from Serreze et al. (2006) with some modifications (see Section 2.1).
[b] See Sections 2.2 and 2.3.
[c] See Section 4 and Vavrus et al. (2012). These projections are uncertain.
[d] Seasonal sea ice is the winter minus summer sea ice volume (Fig. 3).
[e] Multiyear sea ice is the sea ice volume at the end of the summer melt season (Fig. 3).
[f] See Section 2.4.2.
[g] Including the Fram Strait deep water and West Spitsbergen Current.

10,000 km^3 freshwater is stored as Arctic sea ice. This number is probably too low, at least for a climatology representing the late 20th century. Consider replacing the Serreze et al. (2006) ice thickness estimate of 2 m with 3 m, Aagaard and Carmack's (1989) value and very similar to the estimate of 3.1 m for 1958–1976 by Rothrock et al. (1999). The annual-mean freshwater storage estimate in sea ice is then about 15,000 km^3, which is much closer to the Aagaard and Carmack (1989) estimate of 17,300 km^3. As shown below in Section 2.3, the volume of sea ice formed each year is around 13,000 km^3 (for 1980–2000), most of which melts without leaving the Arctic (Section 3.1.1). A fraction of this seasonal sea ice survives the summer melt to become multiyear ice, or is exported south.

Freshwater is supplied to the Arctic by three principal mechanisms: runoff, oceanic inflow, and precipitation minus evaporation (P − E). Most important, runoff from rivers, streams, and groundwater discharge supplies around 3900 ± 390 km^3 yr^{-1} (assuming 10% error; see below) for 1980–2000 to the Arctic, CAA, and Baffin Bay.[5] This number is the average of two estimates: First, the runoff from the ERA-INTERIM atmospheric reanalysis product (Dee et al., 2011) is 4200 km^3 yr^{-1} (see Lindsay et al. (2014) for a comparison of reanalysis precipitation products, including ERA-INTERIM). Second, the estimate from river discharge observations, extrapolated to fill the substantial data gaps, is 3600 km^3 yr^{-1}. This value is derived from the data shown by Shiklomanov (2010) (his Fig. R1) and adjusted to exclude the Yukon River (about 200 km^3 yr^{-1}) and include the contributions from the CAA and Baffin Bay (which add about 500 km^3 yr^{-1} more). The average of these two estimates equals 3900 ± 390 km^3 yr^{-1} (assuming 10% error), and is reported in Table 1 and Fig. 2 as the 1980–2000 mean runoff. This number exceeds that of Serreze et al. (2006) (3200 ± 320 km^3 yr^{-1}) for two reasons: First, the present synthesis includes the Arctic and the CAA as far as Davis Strait, not just the Arctic. Second, the Serreze et al. (2006) value comes from observations of river discharge only. The difference between the estimates from ERA-INTERIM and the discharge data reflects the combined uncertainty in estimating freshwater runoff from reanalysis products and direct measurements. This error, about 10%, amounts to 390 km^3 yr^{-1} in the 1980–2000 runoff estimate. It is consistent with Lindsay et al.'s (2014) estimate of a positive bias in the ERA-INTERIM precipitation fields of about the same size (their Fig. 3b).

The flow through Bering Strait is the next largest source of liquid freshwater, supplying around 2400 ± 300 km^3 yr^{-1} relative to S_{ref} = 34.80 (Woodgate and Aagaard, 2005; Serreze et al., 2006). This estimate is based on direct observations for 1990–2004 of the main-channel flow which accounts for about 1700 km^3 yr^{-1}. An additional 700 km^3 yr^{-1} is added to account for the Alaskan Coastal Current and freshwater flux due to seasonal stratification which were not observed throughout this period. Estimating the 1980–2000 average flux is hard because the only years with adequate observations are 1991, 1998, and 1999. In the absence of other data, we quote 2400 ± 300 km^3 yr^{-1} in Table 1, mindful of this uncertainty. The Bering Strait ice flux is small in comparison, adding another 140 ± 40 km^3 yr^{-1} freshwater into the Arctic (Travers, 2012) in 2007, for example.

Finally, the difference between precipitation and evaporation over the region delivers a net flux of around 2000 ± 200 km^3 yr^{-1} (from ERA-INTERIM; the 10% error is based on the runoff error above). Noting that about 200 km^3 yr^{-1} is added over the CAA and Baffin Bay, this estimate is 10% smaller than the ERA-40 (Uppala et al., 2005) value of Serreze et al. (2006).[6] Input of glacial ice as icebergs or glacial melt

[5] We express freshwater fluxes in km^3 yr^{-1}. To convert to a flux in Sverdrups (Sv) note that 1000 km^3 yr^{-1} equals 31.7 mSv (1 Sv is 10^6 m^3 s^{-1}). Component fluxes are significantly affected by different choices of reference salinity S_{ref}, but the net flux for an enclosed region is not: see Tsubouchi et al. (2012) for a discussion of the effects of choosing different S_{ref}.

[6] It is also derived from the stored reanalysis output fields, rather than the so-called aerological method (Serreze et al., 2006).

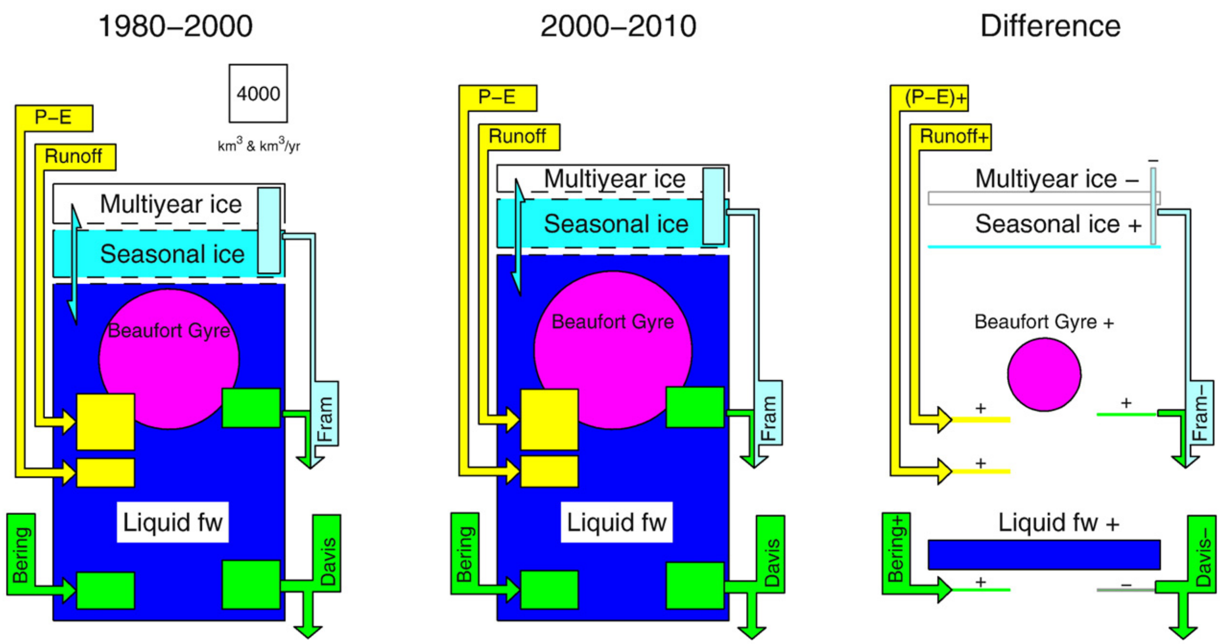

Fig. 2. Schematic Arctic/CAA freshwater budgets. The main reservoirs and fluxes are shown with area proportional to the reservoir volume and the integrated flux in one year, respectively (see the white box for scale). That is, reservoirs: liquid freshwater (fw), freshwater stored as seasonal ice and multiyear ice; the liquid freshwater content of the Beaufort Gyre is shown with the circle. Incoming fluxes: precipitation minus evaporation (P − E), runoff, and Bering Strait ocean currents. Outgoing fluxes: Fram Strait (liquid and in sea ice) and Davis Strait. The left panel represents the era before significant Arctic environmental change (1980–2000). The middle panel represents the last decade, and the right panel shows the differences between two periods. The reference salinity is 34.80. See also Fig. 4 and Table 1.

water into the Arctic and Baffin Bay is relatively small, around 330 ± 20 $km^3\ yr^{-1}$, from Bamber et al.'s (2012) estimates. Summing each of these sources (Table 1), the total freshwater supply is about 8800 ± 530 $km^3\ yr^{-1}$.

Freshwater also leaves the Arctic as oceanic liquid freshwater and sea ice. The most important liquid freshwater export route is via the CAA and Baffin Bay at around 3200 ± 320 $km^3\ yr^{-1}$ through Davis Strait (sea ice adds about 160 km^3 freshwater each year; Serreze et al. (2006)). This estimate is inherently uncertain, however, because it is based on 1998–2000 data of the flux at Barrow Strait, not Davis Strait. These observations are then multiplied by a factor of 2–3, from models, to estimate the Davis Strait flux. In comparison, direct measurements of Davis Strait flux were made between 1987 and 1990 using a moored array (Cuny et al., 2005), although the shelves and the upper 150 m were excluded. The liquid freshwater flux was 2900 ± 1100 $km^3\ yr^{-1}$, extrapolating to estimate the unobserved parts, which is insignificantly different from the 3200 ± 320 $km^3\ yr^{-1}$ number quoted above.

Export of both liquid freshwater and sea ice through Fram Strait is also important. The liquid freshwater flux through Fram Strait is around 2700 ± 530 $km^3\ yr^{-1}$, while export of freshwater as sea ice in Fram Strait is about 2300 ± 340 $km^3\ yr^{-1}$ (Serreze et al., 2006). The 2700 ± 530 $km^3\ yr^{-1}$ Fram Strait liquid freshwater flux includes the contributions from the deep water and the West Spitsbergen Current. Freshwater flux across the Barents Sea Opening is relatively weak, −90 ± 90 $km^3\ yr^{-1}$, compared to $S_{ref} = 34.80$ because inflowing salty Atlantic water compensates the inflowing fresh Norwegian coastal current.

The total freshwater export rate for the Arctic, CAA, and Baffin Bay thus sums to about 8700 ± 700 $km^3\ yr^{-1}$ (including the small flux of about 200 $km^3\ yr^{-1}$, of unknown accuracy, through Fury and Hecla straits based on Straneo and Saucier, 2008). This flux balances the freshwater sources with a discrepancy that is indistinguishable from zero within the large uncertainty: the residual is about 100 ± 900 $km^3\ yr^{-1}$ leaving the Arctic (Table 1).

This budget, mainly from Serreze et al. (2006), nominally covers the period 1980–2000, roughly speaking before major adjustment in the Arctic hydrological cycle. Since publication of Serreze et al. (2006), results from several studies have updated our knowledge of the Arctic freshwater system and how it appears to have changed in the last decade. We now discuss these changes.

2.2. Rapid increase in liquid freshwater storage since 2000

The storage of freshwater in the Arctic Ocean is increasing. The first indication of departure from the climatology of Serreze et al. (2006) was provided by Proshutinsky et al. (2009). Using data collected in 2003–2007 and historical observations, they found that the freshwater content in the Beaufort Gyre increased by over 1000 km^3 relative to the pre-1990s climatology. The 1990s were also found to be fresher than the climatology of the previous decades. The freshening apparently accelerated during the late 2000s: McPhee et al. (2009) found that the freshwater content had increased by 8500 km^3 in the Canada and Makarov basins by 2008. This increase is measured relative to winter climatology (PHC 3.0), and uses extensive aerial surveys carried out in March–April 2008. For comparison, it corresponds to about one year's worth of import (and export) of freshwater in the 1980–2000 budget discussed in Section 2.1.

The rapid freshening is evident in other datasets as well. Rabe et al. (2011) used summer salinity profiles from ships, drifting ice stations and autonomous stations between 2006 and 2008 to estimate the freshwater content for the entire Arctic Ocean with a bottom depth deeper than 500 m. Compared to summer salinity profiles obtained during the period 1992–1999, they found that the freshwater content had increased by 8400 ± 2000 km^3 (in this case relative to $S_{ref} = 35.00$). The freshwater content m (Eq. (1)) increased across nearly all of the Arctic between 2006–2008 and 1992–1999. Although the estimated freshwater content increases of McPhee et al. (2009) and Rabe et al. (2011) are similar, one should keep in mind that they are not directly comparable. The two estimates cover different regions, different times

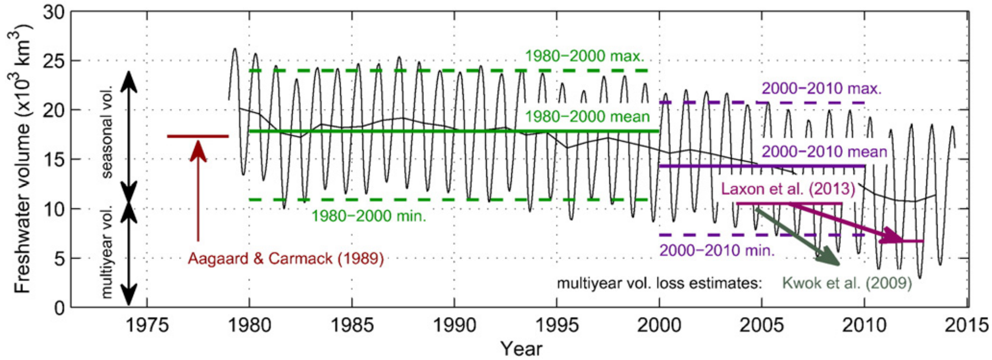

Fig. 3. Freshwater volume stored as Arctic sea ice from the PIOMAS assimilation product (Zhang and Rothrock, 2003). The thin full lines show the seasonally-varying and annual average values. The averages of the minimum (summer) and maximum (winter) volumes are shown with thick dashed lines for the periods 1980–2000 and 2000–2010. Thick full lines show the averages over these periods. The seasonal and multiyear volumes of freshwater stored as ice are shown, from PIOMAS, as is the early average volume estimate of Aagaard and Carmack (1989). The estimates of the recent loss of freshwater from multiyear sea ice by Kwok et al. (2009) and Laxon et al. (2013) are shown with arrows. See Table 1 and Fig. 2.

of the year, are based on different time periods, and use different reference salinities and different lower levels of integration (McPhee et al., 2009 integrated from the depth of the 34.80 isohaline surface, whereas Rabe et al. (2011) integrated from the depth of the 34.00 surface: see Eq. (1)).[7] Despite these differences, the conclusion is the same; the Arctic liquid freshwater content increased rapidly during the 2000s by about 10%. Our estimate of the 2000–2010 average liquid freshwater volume is therefore 101,000 km^3 (Table 1; see also Fig. 7 below).

The findings of McPhee et al. (2009) and Rabe et al. (2011) were corroborated by Giles et al. (2012), who used satellite measurements between 1995 and 2010 to show that the dome in sea level associated with the Beaufort Gyre inflated and the sea level slope steepened at the edges. They estimated that this inflation corresponds to an increase in freshwater storage of 8000 ± 2000 km^3 in the western Arctic Ocean. Rabe et al. (2014) also recently report that over the period 1992–2012 the liquid freshwater content increased at an average rate of 600 ± 300 km^3 yr^{-1}.

The cause of the inflation, freshening, and increased storage in the 2000s is a wind-driven strengthening of the Beaufort Gyre (see Section 3 below for an explanation of this mechanism). The extra freshwater is, at least in part, redistributed from other parts of the Arctic. For example, Morison et al. (2012) used a combination of hydrochemistry, hydrography and satellite altimetry and bottom pressure measurements to show that over the period 2005–2008 the dominant liquid freshwater content changes involved an increase in the Canada Basin compensated by a decrease in the Eurasian Basin. The upper waters of the Canada Basin were 1–3 practical salinity units fresher in 2008 than the pre-1990s climatology and 1–2 units saltier in the Makarov Basin. The changes were found to be due to a re-routing of Siberian river runoff associated with changes in the phase of the Arctic Oscillation (see Sections 2.5 and 3.1.2).

2.3. Sea ice changes since 2000

Sea ice is the component of the Arctic freshwater cycle with most rapid change. Sea-ice extent is declining, especially in summer. For example, Vaughan et al. (2013) show that the linear trend in northern hemisphere monthly-mean sea ice extent is −3.8 ± 0.3% per decade for the period November 1979 to December 2012 (considering all months). The corresponding trends for winter, spring, summer, and autumn are −2.3 ± 0.5%, −1.8 ± 0.5%, −1.6 ± 0.8%, and −7.0 ± 1.5%, respectively. These figures show that the decline in sea ice extent is dominated by loss in summer and autumn. The September sea ice extent reached record-breaking values of 4.3 × 10^6 km^2 in 2007 and 3.6 × 10^6 km^2 in 2012 (the 1979–2001 average is 7.0 × 10^6 km^2).

Sea-ice thickness is also declining. For example, Kwok and Rothrock (2009) show that the average ice thickness at the end of the melt season was 3.02 m during the period 1958–1976 (based on submarine data), but just 1.43 m during 2003–2007 (based on ICESat satellite data). Similarly, Comiso (2012) shows that the trend in the extent of multiyear sea ice — which is thicker than first-year ice — is −16% for 1981–2011 (measured by satellite during winter). This is a faster rate of decline than for sea ice extent as a whole (−3.8 ± 0.3% per decade, from above), reflecting the preferential reduction of thick, multiyear ice and hence a decline in average thickness.

Concomitant with the declines in sea-ice extent and thickness, sea-ice volume is shrinking. Perhaps the best estimates of sea-ice volume changes over the last 30 years are from Arctic assimilation products, such as the Polar Science Center Pan-Arctic Ice Ocean Modeling and Assimilation System (PIOMAS; Zhang and Rothrock, 2003). The PIOMAS assimilates ice concentration and sea-surface temperature data, and its sea-ice thickness estimates are validated against satellite products and upward-looking sonars on moorings and submarines. Nevertheless, uncertainty remains in the PIOMAS product, especially for the absolute ice volume numbers. Fig. 3 shows that between 1980 and 2000 the mean PIOMAS freshwater volume stored in sea ice is 17,800 km^3, very similar to the Aagaard and Carmack (1989) estimate of 17,300 km^3, and the number quoted in Table 1. The PIOMAS freshwater volume stored as multiyear ice for 1980–2000 is 10,900 km^3 and the seasonal sea ice is 13,000 km^3 (Table 1). For the decade 2000–2010, the PIOMAS annual mean freshwater volume stored in ice decreased to 14,300 km^3 (with 7400 km^3 as multiyear and 13,400 km^3 as seasonal ice). This loss of freshwater stored in multiyear ice agrees, more or less, with the satellite-based estimate of Kwok et al. (2009). For 2011 the PIOMAS estimate of annual mean freshwater volume in sea ice is 10,900 km^3, a loss of about 40% compared to the 1980–2000 period. This value accounts for both sea-ice thinning and sea-ice extent reduction and is similar to Laxon et al.'s (2013) satellite-based estimate (Fig. 3).

2.4. Freshwater fluxes since 2000

Section 2.1 discusses 1980–2000 conditions. A more updated account on exchanges through the main oceanic gateways between the

[7] We can estimate the impact of the last two factors: Rabe et al.'s (2011) choice of S_{ref} = 35.00, not 34.80, makes their estimate of the liquid freshwater content *larger* because one integrates a greater salinity anomaly in Eq. (1). Their choice of the 34.00 surface, not the S_{ref} surface, as the starting point for integration makes their estimate *smaller* because one integrates over a smaller part of the halocline. These two choices have compensating influence on estimates of freshwater inventory. Using the PHC 3.0 climatology we compute that the net effect is a decrease of 1000 km^3 in the *total* freshwater volume. Presumably the effect on the *anomaly* in freshwater volume is less and well within Rabe et al.'s (2011) error bars.

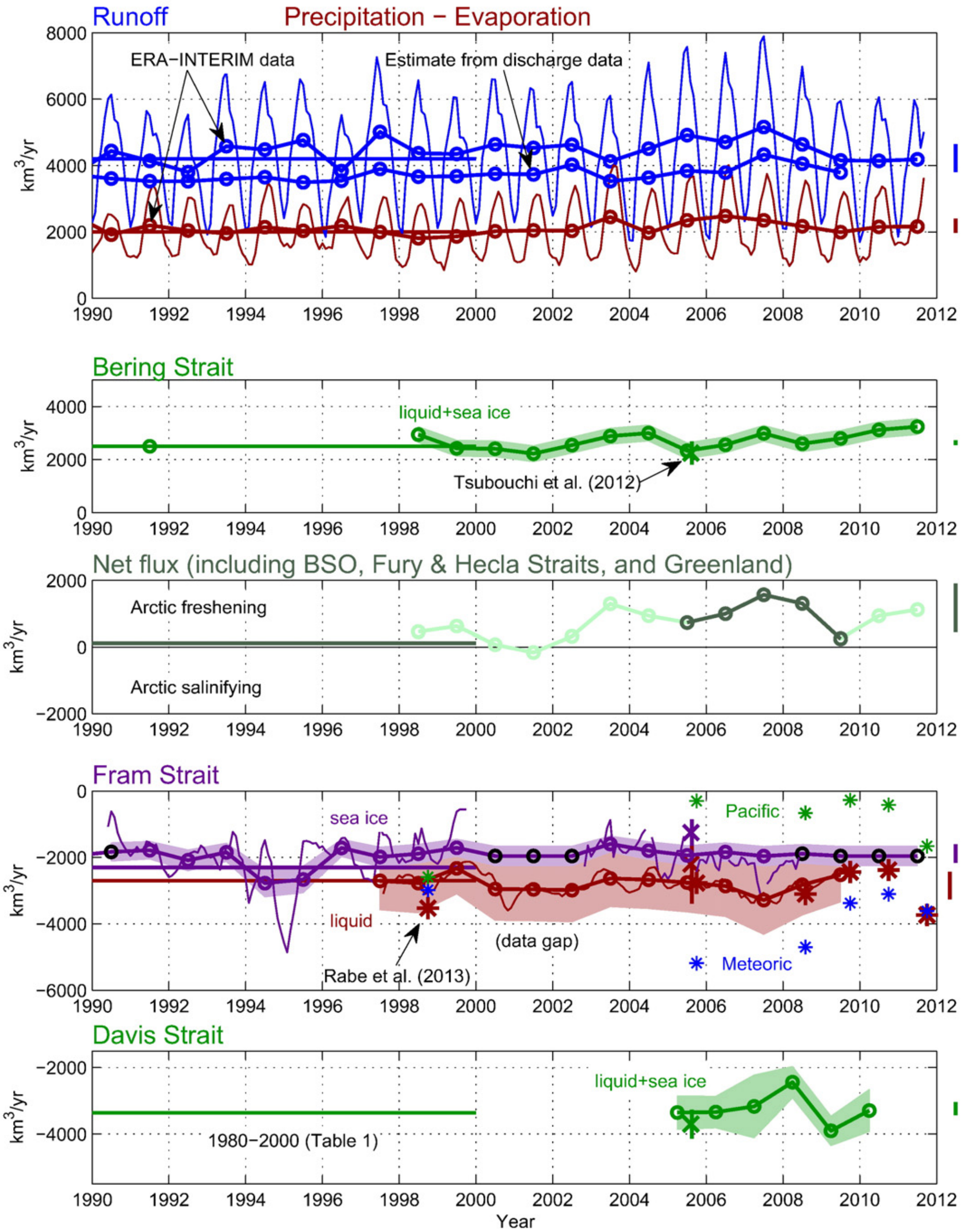

Fig. 4. Synthesis of ocean freshwater flux time series. The upper panel shows runoff and precipitation minus evaporation (P − E) from the ERA-INTERIM reanalysis. An estimate from the river discharge data of Shiklomanov (2010) is also shown (see text). The second panel shows Bering Strait fluxes from Woodgate et al. (2012). The fourth panel shows fluxes as liquid and stored in sea ice through Fram Strait from de Steur et al. (2009) and Spreen et al. (2009). The bottom panel shows Davis Strait fluxes from Curry et al. (2014). The middle panel shows the net freshwater flux (positive means Arctic freshening) and includes the relatively minor Barents Sea Opening (BSO), Fury, Hecla and Greenland fluxes (light color indicates some missing components). Circles indicate annual mean values with error bars on the 2000–2010 mean values at the right hand side. Shading indicates uncertainties on the annual averages, where available. The data gaps in the Fram Strait sea ice record (black) are filled by reverting to the average seasonal cycle. The values from the 1980 to 2000 budget in Table 1 are shown with lines on the left. The crosses show the quasi-synoptic flux estimates for summer 2005 from Tsubouchi et al. (2012). The stars show the Fram Strait flux estimates from Rabe et al. (2013) including the contributions from Pacific and meteoric waters. See also Fig. 2.

Arctic Ocean and the subpolar seas is provided by Beszczynska-Möller et al. (2011). Tsubouchi et al. (2012) present a pan-Arctic flux estimate using mainly hydrographic data and dynamical constraints, plus some mooring data (relative to $S_{\mathrm{ref}} = 34.66$). Their estimate is quasi-synoptic because it represents the 32-day period 9 August to 10 September 2005, and so is useful for comparison. Here we discuss the latest numbers in turn, including variability and trends (see also Fig. 4).

2.4.1. Runoff and precipitation minus evaporation

Precipitation over the Arctic has increased in recent years, according to both atmospheric reanalysis and coupled climate models. For example, using the ERA-INTERIM product, both runoff into, and P − E over, the Arctic and CAA were greater in the 2000s than for 1980–2000. Runoff was around 4600 km^3 yr^{-1} for 2000–2010 compared to 4200 km^3 yr^{-1} for 1980–2000 (long-term terrestrial storage effects are small so runoff changes derive from precipitation changes over land).

Similarly, using the adjusted river discharge data from Shiklomanov (2010) to estimate runoff change, we find an increase from 3600 to 3800 $km^3\ yr^{-1}$ between two periods. Taking the average of these two estimates gives our estimate of 4200 ± 420 $km^3\ yr^{-1}$ (Table 1). We roughly estimate the uncertainty in this value to be 10%, based on the differences between the discharge data and the ERA-INTERIM reanalysis. ERA-INTERIM P − E was around 2200 ± 220 $km^3\ yr^{-1}$ for 2000–2010 compared to 2000 ± 200 $km^3\ yr^{-1}$ for 1980–2000 (also assuming 10% errors; see Table 1 and Section 2.1). Freshwater flux from Greenland is also higher; about 370 ± 25 $km^3\ yr^{-1}$ rather than 330 $km^3\ yr^{-1}$ (Bamber et al., 2012).

It is hard to be sure if these increases in runoff and P − E are real or not. They are both smaller than the nominal uncertainty in Fig. 4 of ±10%, based on the differences between the ERA-INTERIM and ERA-40 runoff and P − E numbers quoted in Section 2.1. Nevertheless, the ERA-INTERIM product is among the best available. It is one of three out of seven reanalysis products that Lindsay et al. (2014) identify as being more consistent with independent observations. They compare the ERA-INTERIM precipitation field with the gridded monthly Global Precipitation Climatology Centre Full Data Reanalysis Version 5 (Rudolf et al., 2010). They find that ERA-INTERIM performs best of all seven models considered in matching the observed precipitation anomalies (the correlation coefficient is slightly less than 0.8). The ERA-INTERIM P − E product is therefore a good choice for our purposes. Moreover, climate models predict increasing precipitation and runoff during the 21st century. For example, Vavrus et al. (2012) estimate precipitation increases about 40%, on average, from an ensemble of CCSM4 projections (see Section 4.1). Therefore, we suspect that the Arctic precipitation did indeed increase between 1980 and the 2000s. To our knowledge, no study exists that compares Arctic precipitation data from the 2000s with earlier decades, however.

2.4.2. Bering Strait

The Bering Strait import of Pacific (liquid) freshwater amounted to 2500 ± 630 $km^3\ yr^{-1}$ over the period 1999–2005 (Woodgate et al., 2006). Bering Strait volume flux increased from 0.7 Sv (22 × 10^3 $km^3\ yr^{-1}$) in 2001 to 1.1 Sv (35 × 10^3 $km^3\ yr^{-1}$) in 2011 with insignificant change in salinity (Woodgate et al., 2012). In consequence, the freshwater flux increased from around 2000–2500 $km^3\ yr^{-1}$ in 2001 to 3000–3500 $km^3\ yr^{-1}$ in 2011 (Fig. 4). The year 2001 exhibited the lowest freshwater flux at 2200 $km^3\ yr^{-1}$ in the period 1998–2011, however. Compared to the uncertainty in the freshwater flux estimate (around 250–500 $km^3\ yr^{-1}$) the 2001 to 2011 increase in Bering Strait freshwater flux is significant. In Table 1 and Fig. 1 we estimate the 2000–2010 Bering Strait liquid flux to be 2500 ± 100 $km^3\ yr^{-1}$. This decadal average is indistinguishable from the estimate of 2400 $km^3\ yr^{-1}$ which, in the absence of a complete data record, we take as the best-available, likely poor, value for the period 1980–2000 (Section 2.1). Tsubouchi et al.'s (2012) quasi-synoptic estimate of the Bering Strait flux for summer 2005 is 2300 ± 400 $km^3\ yr^{-1}$, close to the annual average of Woodgate et al. (2012) for that year.

2.4.3. Fram Strait

The export of liquid freshwater in the East Greenland Current in Fram Strait was 1960 ± 760 $km^3\ yr^{-1}$ over the period 1997–2008 (de Steur et al., 2009). The 2000–2010 average was nearly 2100 $km^3\ yr^{-1}$, using an improved method by de Steur et al. (2014) to fill data gaps. These estimates, from moorings and model results, exclude the West Spitsbergen Current which carries warm salty water polewards. From the perspective of the budget this flow counts as a southward flux of freshwater relative to $S_{ref} = 34.8$. Serreze et al. (2006) estimate it exports 760 ± 320 $km^3\ yr^{-1}$ which gives a net of around 2800 ± 420 $km^3\ yr^{-1}$ for Fram Strait liquid freshwater flux (for years 2000–2010; Fig. 4). This number is essentially unchanged from the 1980 to 2000 value of 2700 $km^3\ yr^{-1}$ (Table 1, Fig. 2). Tsubouchi et al.'s (2012) quasi-synoptic estimate of 2200 $km^3\ yr^{-1}$ for the summer of 2005 is noticeably smaller although within error bars. de Steur et al. (2009) report that Fram Strait liquid freshwater flux is lowest in summer, so seasonal variability is the likely explanation for the difference. Rabe et al. (2013) also provide liquid freshwater flux estimates (stars in Fig. 4).[8] They are based on six summer-time ship sections and current meter data and agree with the de Steur et al. (2009) values. The Rabe et al. (2013) flux estimate for summer 2011 is 3900 $km^3\ yr^{-1}$, noticeably larger than the previous 14 years, however, due to a greater Pacific Water contribution.

The Fram Strait export of sea ice is estimated to have carried 2100 $km^3\ yr^{-1}$ freshwater averaged over the winters of 2003–2008 (winters are defined as October through May; Spreen et al., 2009). The annual average for 2000–2010 (1990–2000) is 1900 ± 280 (2000 ± 290) $km^3\ yr^{-1}$ when data gaps are filled using the average seasonal cycle (Fig. 4). The quasi-synoptic value quoted by Tsubouchi et al. (2012) is 1250 $km^3\ yr^{-1}$ for summer 2005. This number is about half of the annual average, but is unexceptional in light of the annual cycle in sea ice flux reported by Vinje et al. (1998) and visible for some years in Fig. 4. For the period 1990–1999, Kwok et al. (2004) estimate the freshwater flux in sea ice to be 1800 $km^3\ yr^{-1}$. Their estimate is significantly lower than that of Serreze et al. (2006) (2300 ± 340 $km^3\ yr^{-1}$, based on Vinje et al. (1998)), but it is unclear which is more accurate. Given the large inter-annual variability in sea ice flux (400 $km^3\ yr^{-1}$ according to Kwok et al. (2004)), and the challenge in observing this variable, there is no evident change in Fram Strait sea ice flux (Spreen et al., 2009).

It is interesting that the Fram Strait sea ice flux is apparently unchanged. Changes have been observed in Fram Strait sea ice properties however. During the 2000s the modal thickness of multiyear sea ice in Fram Strait decreased by approximately one third compared to the 1990s (Hansen et al., 2013). In the 1990s the mean sea ice thickness was 3.4 m; for 2005–2010 it had decreased to 2.5 m with a record low of just 2.0 m in winter of 2010. These changes are consistent with the strong decline of (thick) multiyear sea ice in the Arctic as discussed in Section 2.3. As the total freshwater flux (and its liquid and solid components) has not been observed to change, a decrease in sea-ice thickness is consistent with an increase in the area of sea ice exported. Kwok (2009) and Kwok et al. (2013) report no significant trend in sea ice area export through Fram Strait since 1980, however, albeit with significant inter-annual variations. A possible explanation is that the correlation in sea ice speed through Fram Strait and sea ice thickness has increased (so that more thick ice is exported than before even though thick ice is less abundant). Alternatively, the absence of evident change in Fram Strait sea ice area and volume fluxes, despite declining sea ice thickness, could be explained by observing uncertainty.

2.4.4. Davis Strait

For the period 2004–2010, Curry et al. (2014) report 2900 ± 190 $km^3\ yr^{-1}$ liquid freshwater flux and 320 ± 45 $km^3\ yr^{-1}$ freshwater flux in sea ice. In the absence of other data, we assume these values represent the decade of the 2000s. They include the flux through the whole CAA because the flux south of Baffin Island through Fury and Hecla straits, and hence through Hudson Strait, is negligible in comparison (about 200 $km^3\ yr^{-1}$ according to Straneo and Saucier (2008)). No significant trend exists in the Davis Strait freshwater flux over 2004 to 2010, nor a significant difference from the 1980 to 2000 average of 3400 $km^3\ yr^{-1}$ for both liquid freshwater and ice (Section 2.1). Nevertheless, the 2004–2010 liquid freshwater flux is significantly smaller than the 1987–1990 average for the central part of the Strait: Curry et al. (2014) estimate the 1987–1990 liquid flux to be 4500 ± 730 $km^3\ yr^{-1}$ for this region, but just 3300 ± 220 $km^3\ yr^{-1}$ for 2004–2010. The corresponding quasi-synoptic estimate from

[8] The Rabe et al. (2013) flux numbers are decreased by 5% to account for their higher reference salinity from Table 1 of de Steur et al. (2009).

Tsubouchi et al. (2012) for summer of 2005 is 3700 $km^3\ yr^{-1}$, similar to these longer-term averages and consistent with the 2005 data shown in Fig. 4.

2.4.5. Sources of uncertainty

All of these flux numbers are uncertain. These uncertainties are quoted where possible from the original references or based on intuition from detailed knowledge of the primary observations involved. The uncertainties on the 2000–2010 average fluxes appear in Fig. 4 as vertical error bars on the right hand side. Where flux error estimates are available on annual averages, they are shown with shading. The sources of uncertainty are discussed here.

Uncertainties in estimates of meteoric freshwater supply to the Arctic, either as precipitation or runoff, stem from uncertainty in atmospheric reanalysis products. In particular, precipitation estimates are not well known. For example, the estimates of P − E from reanalysis output fields are lower than those from the aerological method (Serreze et al., 2006), at least for the MERRA model (by about a third; Cullather and Bosilovich, 2011). This result suggests that our P − E estimates are biased low. Lindsay et al.'s (2014) analysis finds that ERA-INTERIM precipitation is biased high, however, as mentioned in Section 2.1. An assessment of Arctic precipitation estimates from ERA-INTERIM that compares the reanalysis output fields with the aerological method is needed. Comparison with direct precipitation observations is also needed. Measuring solid precipitation is challenging, however, and local variability can make interpreting sparse station data difficult (Lindsay et al., 2014). Therefore, the 10% P − E error in Table 1 is a provisional estimate.

For the oceanic fluxes, there are several sources of error: First, moored instruments are threatened by ice. Often, the salinity of the upper 50 m of the water column is not monitored because sea ice ridges extend down tens of meters. In those cases, significant anomalies in freshwater flux associated with near-surface salinity changes are missed. Moreover, icebergs threaten shelf moorings, especially in Davis Strait. Second, a significant flux occurs over the broad East Greenland Shelf in Fram Strait (270 km wide) of which only a small part is monitored with the mooring array. This flux is estimated to be 800 ± 400 $km^3\ yr^{-1}$ (from a numerical model; de Steur et al., 2009). Third, the short intrinsic spatial scales in the velocity and hydrography fields (the baroclinic deformation radius) mean that moorings must be closely spaced to obtain reliable total fluxes by interpolation. Obstructed access, due to heavy ice or clearance issues in territorial waters, is also a problem that makes deploying or recovering moorings harder and leads to gaps in coverage. The calculation of annual averages is vulnerable to data gaps because most of the component fluxes show large seasonal cycles (Fig. 4; the averages reported here are for a calendar year whenever possible). Similarly, inter-annual variations are also typically large and missing data make decadal averages uncertain. For the same reason, quasi-synoptic estimates, like that of Tsubouchi et al. (2012), do not represent decadal average fluxes accurately.

Efforts to reduce these errors continue and substantial progress has been made in the last 15 years. Two developments are particularly noteworthy. Developments in oceanographic instrument technology now permit continuous flux monitoring efforts in many ice-covered straits. For example, moored winch systems (such as the ICECYCLER; Fowler et al., 2004) can provide temperature and salinity profiles in the upper part of the water column. An acoustic warning system detects and avoids sea ice and thus prevents damage to the sonde. Other designs are passive (such as the ISCAT; Beszczynska-Möller et al., 2011) and are designed to survive being pushed down by the ice. They measure in the upper water column and have been used in strong currents, for example in Bering Strait, which can defeat moored winches. These systems make it possible to determine the freshwater content close to the surface, where it is concentrated, and improve estimates of freshwater flux. Seagliders, autonomous vehicles that measure hydrographic properties among other variables, are now capable of operating under ice (Webster et al., 2014). They are used in wide deep passages that cannot be monitored effectively with traditional moorings. The under-ice capability expands the coverage so that fluxes in Davis and Fram straits can be observed on the shelves. Seagliders are unable to operate effectively in shallow straits with strong currents, however, such as Bering Strait. The second noteworthy development concerns numerical circulation models of the Arctic and sub-Arctic seas. They have gained resolution and fidelity since the end of the last century. Models now include processes and dynamical scales relevant to observational oceanographers (for a recent review of Arctic models see Proshutinsky et al., 2011). Realistic models are used to fill data gaps, quantify variability, for instance in freshwater fluxes, and elucidate the causes of change. Examples include the PIOMAS model mentioned in Section 2.1 and de Steur et al.'s (2009) use of the North Atlantic/Arctic Ocean Sea Ice Model to fill the East Greenland shelf data gap mentioned above.

2.5. Freshwater origins and pathways

Along with salinity, measurements of chemical tracers, such as nitrate, phosphate, oxygen isotopes and alkalinity, reveal the origins of different freshwater sources in the Arctic. Contributions from Pacific Water, meteoric water (runoff and precipitation) and sea-ice melt can all be estimated, as can their changes over time (Schlosser et al., 1994, 1995; Bauch et al., 1995). Pacific Water and river water dominate in the Canadian Basin although their contributions vary. Pacific Water entering through the Bering Strait is found throughout the Canadian Basin. Its spread is bounded by two paths: across the central Arctic with the Transpolar Drift or east along the boundary (Jones et al., 1998; Steele et al., 2004, see also Section 3.1.2). Meteoric water consists mostly of river water arriving from the Laptev Sea and East Siberian Shelves and flows polewards near the Lomonosov and Mendeleyev ridges (Ekwurzel et al., 2001). Pacific Water can be found down to 300 m depth in the southern Beaufort Gyre while river water occurs mostly in the upper 50 m (Jones et al., 2008). Melt water from sea ice is only found in summer in a surface layer: in the halocline there is a negative melt water contribution indicating brine formation from freezing (Macdonald et al., 2012).

In the early 1990s the front between Pacific and Atlantic derived waters shifted east from the Lomonosov to the Mendeleyev Ridge. Ekwurzel et al. (2001), McLaughlin et al. (1996) and Swift et al. (2005) discuss evidence of earlier variations. This shift is associated with a change from anticyclonic to cyclonic circulation (Section 3.1.2). By 2004 the front had shifted back to the Lomonosov Ridge, returning Pacific Water to the central Arctic (Alkire et al., 2007). Moreover, from the first half of the 1990s to 2005 the inventory of runoff water in the central Arctic increased (Jones et al., 2008; Newton et al., 2013). Data from the 1980s to 1990s show a tight relation between river water and brine which suggests a common source on the continental shelves. By 2005 this relation had broken down, likely associated with the general retreat of summer sea ice (Section 2.3) so that brine production from freezing now also occurs in the central Arctic (Newton et al., 2013).

Freshwater leaving the Arctic through the CAA consists mostly of Pacific Water (Rudels and Friedrich, 2000; Jones et al., 2003). The total volume flux through the Archipelago is about twice, perhaps even more, as large as the Bering Strait inflow, however (see Table 1 of Beszczynska-Möller et al., 2011). Therefore, a substantial fraction of Atlantic water must also pass through the CAA and in particular through Nares Strait, the easternmost gap. Bailey (1956) noticed that the deep and bottom water in Baffin Bay has similar properties to the water at 250 m in the Arctic Ocean and proposed that a deep inflow through Nares Strait could be the source. Rudels et al. (2004) showed that the properties of the Baffin Bay deep water are similar to those of the lower halocline in the Canada Basin, which can be traced to the Barents Sea winter mixed layer. Therefore, they suggested that the Barents Sea inflow branch of Atlantic water makes the largest contribution to the CAA outflow, both in the deep outflow and, by mixing with Pacific-derived water, the upper layer outflow to Baffin Bay.

Freshwater leaving through Fram Strait consists mostly of meteoric water (Falck et al., 2005; Jones et al., 2008; Dodd et al., 2009, 2012; Rabe et al., 2013). Brine dominates over sea-ice melt and the Pacific Water contribution is small and variable (Taylor et al., 2003; Falck et al., 2005). Rabe et al. (2013) show that on average 50% less freshwater was extracted by freezing from the water present in Fram Strait in the summers of 2009 and 2010, compared to 2005 and 2008. There was on average 30% less meteoric water in 2009 and 2010 compared to 2005 and 2008. In 2011, nearly four times more Pacific Water contributed to the freshwater flux compared to the average from 2008, 2009, and 2010. There was a similarly high fraction of Pacific Water in 1998. These changes can be seen in Fig. 4 where the Pacific and meteoric water components are plotted (stars) from Rabe et al. (2013).[9] The extra melt and extra Pacific Water that reached Fram Strait are likely related to a freshwater anomaly seen in the Lincoln Sea between 2007 and 2010 (de Steur et al., 2013). Clearly the rates and/or pathways of Arctic freshwater transport are changing: mechanisms behind these changes are discussed in Section 3.1.2.

2.6. Summary of freshwater status and export

Straightforward interpretation of the information in Table 1 suggests the following: Freshwater sources to the Arctic and CAA have increased in the 2000s compared to the 1980–2000 period. Both runoff and P − E have increased by about 10%. The freshwater sources sum to 9400 ± 490 $km^3\ yr^{-1}$ for the 2000s rather than 8800 ± 530 $km^3\ yr^{-1}$ for 1980–2000. The freshwater sinks sum to 8250 ± 550 $km^3\ yr^{-1}$ for the 2000s rather than 8700 ± 700 $km^3\ yr^{-1}$ for 1980–2000. The 1980–2000 budget therefore sums to 100 ± 900 $km^3\ yr^{-1}$ freshening the Arctic; the 2000s budget sums to 1200 ± 730 $km^3\ yr^{-1}$ freshening it.[10] Therefore, these estimates suggest that the Arctic and CAA accumulated an extra 12,000 ± 7300 km^3 freshwater due to unbalanced fluxes over the decade of the 2000s (see also Section 3.4 and Fig. 7 below). In light of the uncertainty, this extra freshening is significant, but not strongly. Maintaining the existing boundary mooring arrays, and adopting the improved observing technologies described in Section 2.4.5 where possible, will likely detect future changes in the Arctic freshwater system.

Another likely explanation for the increased storage in the Beaufort Gyre liquid freshwater reservoir is the smaller sea ice reservoir (Section 2.3). According to chemical tracers in the study by Yamamoto-Kawai et al. (2009), an extra 2.7 m per unit area of sea ice melted in the central Canada basin in 2006 and 2007. Satellite data suggests that melting of multiyear ice in the Beaufort Gyre accumulated up to 1100 km^3 freshwater between 2004 and 2009 (Kwok and Cunningham, 2010). Multiyear ice volume also decreased because of less replenishment from first year ice. Indeed, this is the main reason for recent decreased total sea ice volume. Over the whole Arctic Ocean, freshwater stored as ice dropped by approximately 4300 (2800) km^3 between the autumns (winters) of 2004 and 2008 (Kwok et al., 2009). This extra liquid freshwater is a substantial fraction of the observed increase.

A third possibility exists, albeit less likely: The extra freshwater could come from a redistribution within the Arctic Ocean, driven, for example, by a change in the wind (see Section 3). The studies claiming increased liquid freshwater volume in the western Arctic (Section 2.2) do not comprehensively sample the entire Arctic, CAA, and Baffin Bay. Some type of extrapolation to unsampled areas is unavoidable. Therefore, it is conceivable that freshwater missed in early inventory estimates was sampled and recorded in the decade of the 2000s. In this way, the increase in liquid freshwater reservoir volume could be due to a redistribution from unsampled to sampled areas without there actually being any real change in the total volume. The size of this effect still needs to be quantified.

On this basis, the state of knowledge of the Arctic freshwater budget is as follows (see Figs. 2–4, Table 1, and the cited sections for details):

- Nearly all the Arctic freshwater reservoirs are changing. Liquid freshwater stored in the Arctic is significantly higher in the 2000s compared to 1980–2000 (Section 2.2). Multiyear sea ice storage is lower (Section 2.3). The most uncertain reservoir term is the sea ice volume, reflecting the challenge of measuring sea ice thickness.
- It is hard to detect changes in freshwater fluxes. Nevertheless, general circulation models suggest that precipitation increased for the decade of the 2000s compared to the estimate for 1980–2000 (Section 2.4). Similarly, models and river discharge data show increased runoff. Despite flux increases from 2001 to 2011, it is uncertain if the marine freshwater source through Bering Strait has changed, as observations in the 1980s and 1990s are incomplete. Estimates of Fram Strait sea ice and liquid fluxes are unchanged, within error bars, since measurements began in the 1990s (Section 2.4.3). The ice is thinner and the area export flux is apparently unchanged, however, suggesting that thick ice is being exported faster, or that the ice volume flux has in fact decreased without being detected. The Fram Strait liquid freshwater contains more ice melt. Observations of Davis Strait liquid fluxes are shorter in duration, and show no obvious changes. The liquid freshwater flux in the central part of the strait was reduced by 26% for 2004–2010 compared to 1987–1990, however. The total net freshwater flux to the Arctic has apparently increased in the 2000s compared to 1980–2000 (Fig. 4, Table 1). Measuring oceanic freshwater fluxes remains a challenge although technology now exists for this purpose (Section 2.4.5).
- A shift in the balance of sources and sinks can explain the increase in liquid freshwater stored in the western Arctic although the significance of the shift compared to the total uncertainty is not very high (Section 2.6; see also Section 3.4 and Fig. 7). A smaller reservoir of sea ice is also probably important. Internal redistribution of freshwater and insufficient sampling of the freshwater reservoirs may also contribute to the observed freshwater increase.

3. Freshwater mechanisms

Here we discuss mechanisms relevant to storage and export of freshwater from the Arctic. We consider observations, numerical models and theory, where possible. The overarching question is: What processes govern Arctic Ocean freshwater storage and export?

3.1. Storage and distribution

Mechanisms controlling how Arctic freshwater is stored – as ice or liquid – and distributed in space – both horizontally and vertically – are central to understanding the Arctic's role in the hydrological cycle (Carmack and McLaughlin, 2011). Insight into these mechanisms can be found by first asking, why, in its basic state, is the Arctic Ocean so fresh?

3.1.1. Fresh basic state

As described in Section 2, the sources of Arctic freshwater are river runoff, the influx of fresh surface waters through Bering Strait, and the regional imbalance of P − E. These are relatively large sources. For example, the Arctic basin contains approximately 1% of the global ocean volume, but receives 11% of the global river runoff (Shiklomanov et al., 2000).

[9] The brine contribution to the Fram Strait liquid freshwater flux is not plotted but can be deduced as the (positive) flux that must be added to the Pacific and meteoric fluxes (small stars) to equal the total flux (large stars). The brine contribution equals the amount of freshwater that was extracted by freezing to make sea ice.

[10] The Serreze et al. (2006) budget sums to 700 $km^3\ yr^{-1}$ salinifying the Arctic, but excluded the CAA and used ERA-40 reanalysis product, not ERA-INTERIM which has a greater precipitation estimate.

The total annual supply of freshwater (relative to $S_{ref} = 34.80$) is around 8800 km^3 (Table 1). With a total surface area of 9.7×10^6 km^2 (excluding the CAA and Baffin Bay), this implies that 0.91 m of freshwater is added to the Arctic Ocean each year, similar to high values of P − E in the equatorial Atlantic ocean (Schmitt et al., 1989).

The large seasonal cycle in sea ice also promotes a fresh upper layer. Freezing in winter produces very fresh ice and rejects salt which drains away from the surface as dense brine. Melting in summer returns freshwater to the surface thus distilling, namely un-mixing, the freshwater from the sea (Aagaard and Carmack, 1989). About 13,400 km^3 of freshwater freezes each winter, and about 11,300 km^3 of freshwater is produced by melting each summer, accounting for the fraction that is exported (Table 1). Therefore, about 1.2 m of freshwater is temporarily added to the surface of the Arctic Ocean by melting, on average, each summer.

Moreover, the Arctic is a place where freshwater tends to remain fresh and concentrated in a small part of the water column. The reason is that the density, and thus stratification, of the Arctic Ocean is primarily a function of salinity rather than temperature (a regime referred to as a β-ocean; Carmack, 2007). Therefore freshwater tends to remain near the surface and is vertically separated from underlying saltier waters (Rudels et al., 2004). Indeed, the Arctic halocline is strongly stratified, stronger than the typical subtropical stratification above a few hundred meters depth and stronger in summer than the typical equatorial stratification in the upper 30 m. The strong halocline suppresses mixing. Wind-driven mixing and upwelling are further weakened by ice coverage which reduces the wind's fetch and rate of injection of turbulent kinetic energy. For these reasons turbulent vertical diffusion of heat and salt across the halocline is weak. The vertical diffusivity is around 10^{-6} m^2 s^{-1} in the central Arctic from a salinity analysis by Rudels et al. (1996). This value is ten times larger than the molecular diffusivity of heat and ten times smaller than that observed in the quiescent thermocline of the eastern subtropical Atlantic (Ledwell et al., 1993). Similarly, turbulence measurements in the central Arctic by Fer (2009) imply a halocline diffusivity (of heat) in the range 10^{-6}–10^{-5} m^2 s^{-1}. This range implies a negligible diffusive loss of liquid freshwater content of $O(10^{-3}$–$10^{-2})$ myr^{-1} across the base of the S_{ref} surface, based on the salinity stratification from the PHC 3.0 climatology.

3.1.2. Wind-forced variability

Given that Arctic freshwater exists primarily near the sea surface, the freshwater storage and distribution are strongly influenced by the wind. Here we briefly summarize the main features of Arctic atmospheric flow involved. Then we discuss wind-forced variability distinguishing between the western Arctic and the central and eastern Arctic.

The main mode of variability in the Arctic troposphere is the Arctic Oscillation, or Northern Annular Mode (Thompson and Wallace, 1998).[11] This mode involves sea-level pressure variations that strengthen or weaken the pressure difference between the polar and middle latitudes. The positive phase brings relatively low sea-level pressure to the Arctic and high pressure in mid-latitudes. The Arctic Oscillation is a pressure anomaly pattern that depends mainly on latitude but it is not exactly symmetric about the pole. Instead, the variability in the central and eastern Arctic, and the Nordic Seas, exceeds that in the west (Morison et al., 2012). This asymmetry reflects the mean sea-level pressure field which shows low pressure in the Barents Sea and high pressure in the Canada Basin(Serreze and Barrett, 2011).[12]

The Beaufort High is a prominent anticyclone in mean sea level pressure north of Alaska. A strong Beaufort High is correlated with the summer-time negative phase of the Arctic Oscillation when air pressure is high across the whole Arctic. It is also associated with the Pacific–North American pattern, and (less strongly) with the Arctic dipole anomaly and the Pacific decadal oscillation.[13] The Beaufort High is a center-of-action (that is, a region of high variance) for all these modes of atmospheric variability (Serreze and Barrett, 2011).

Now consider the surface ocean and ice circulation driven by these winds and the impact on freshwater pathways (see also Section 2.5). Fig. 5 (upper panel) illustrates this flow by showing trajectories of surface particles moving with the 1980–2000 average sea ice velocity (from the Polar Pathfinder dataset; Fowler et al. 2013). In the eastern Arctic, including the Barents and Kara Seas, the flow is to the north and/or west. Liquid freshwater and sea ice move into deep water above the Makarov and Eurasian basins forming the Transpolar Drift over the pole towards Fram Strait (see Section 2.5). In the western Arctic the anti-cyclonic Beaufort Gyre is prominent. The surface ocean and ice circulation is mainly aligned with the sea-level pressure contours, consistent with geostrophic flow in the atmosphere and ocean.

This surface circulation varies according to the wind in the central and eastern Arctic (Proshutinsky and Johnson, 1997; Rigor et al., 2002; Rigor and Wallace, 2004; Morison et al., 2012). When the Arctic Oscillation is negative the sea-level pressure is higher across the whole Arctic, but mainly in the east. At these times, Eurasian runoff flows directly into the Transpolar Drift near the Lomonosov Ridge. When the Arctic Oscillation is positive Eurasian runoff flows further east, penetrating the East Siberian Sea, before leaving the continental shelf (Steele and Boyd, 1998).

In the western Arctic the ocean and ice flow is driven into one of two regimes, either cyclonic or anticyclonic (Proshutinsky and Johnson, 1997): The cyclonic regime involves a weak (or absent) Beaufort High sea-level pressure and weakened anticyclonic winds (or a shifting to cyclonic winds; see Fig. 5 left panel). Then, the Ekman convergence rate decreases, the halocline ascends, sea level drops, and isopycnic (isohaline) surfaces flatten. These changes reduce the freshwater volume stored in the weakened Beaufort Gyre. Freshwater is released and redistributed. Some fraction of this redistributed freshwater flows towards the export channels and drains to the Atlantic (Karcher et al., 2005; Condron et al., 2009; Stewart and Haine, 2013).

Also during the cyclonic regime, as during the positive phase of the Arctic Oscillation, Eurasian runoff penetrates further to the east on the shelves and enters the Canada Basin (Steele and Ermold, 2004; Dmitrenko et al., 2008). The Transpolar Drift shifts east towards the Mendeleyev Ridge and directs freshwater stored in the Beaufort Gyre and Canada Basin towards Fram Strait, increasing the fraction of Pacific freshwater exiting there. North American runoff tends to remain on the shelf and exits through the CAA and not east of Greenland (Taylor et al., 2003; Dodd et al., 2009). The summer of 1989 represents this regime (Fig. 5 left panel).

In contrast, the anticyclonic regime is characterized by a strong Beaufort High sea-level pressure and anticyclonic surface winds in the Canada Basin (see Fig. 5 right panel). These winds drive an Ekman convergence of surface freshwater. The halocline in the Beaufort Gyre is depressed deeper, sea level rises up, and the isopycnic (isohaline) surfaces steepen around the edges. In tandem the ocean currents around the edges are stronger leading to a strong Beaufort Gyre. This strengthening is evident as increased sea ice circulation velocity within the Beaufort Gyre (Kwok et al., 2013). These factors cause anomalously large (small) storage of freshwater in the Canada (Eurasian) Basin, as has been seen for the past several years (Section 2.2).

During the anticyclonic regime, as during the negative phase of the Arctic Oscillation, Eurasian runoff flows off the shelves and into the Eurasian Basin and Transpolar Drift near the Lomonosov Ridge (Steele

[11] The Arctic Oscillation is defined by the first empirical orthogonal function (EOF) of non-seasonal sea-level pressure north of 20°N. It is closely related to the North Atlantic Oscillation (NAO) which characterizes the sea-level pressure difference between the Azores High and the Icelandic Low.

[12] The asymmetry is greater in winter than in summer (Ogi et al., 2004).

[13] Loosely speaking, the Pacific–North American pattern is based on a variance analysis of the height of the 500-hPa surface north of 20°N, the Arctic dipole anomaly is the second EOF pattern in polar sea-level pressure, and the Pacific Decadal Oscillation is the leading EOF of North Pacific sea-surface temperature. Serreze and Barrett (2011) provide details and cite the primary literature.

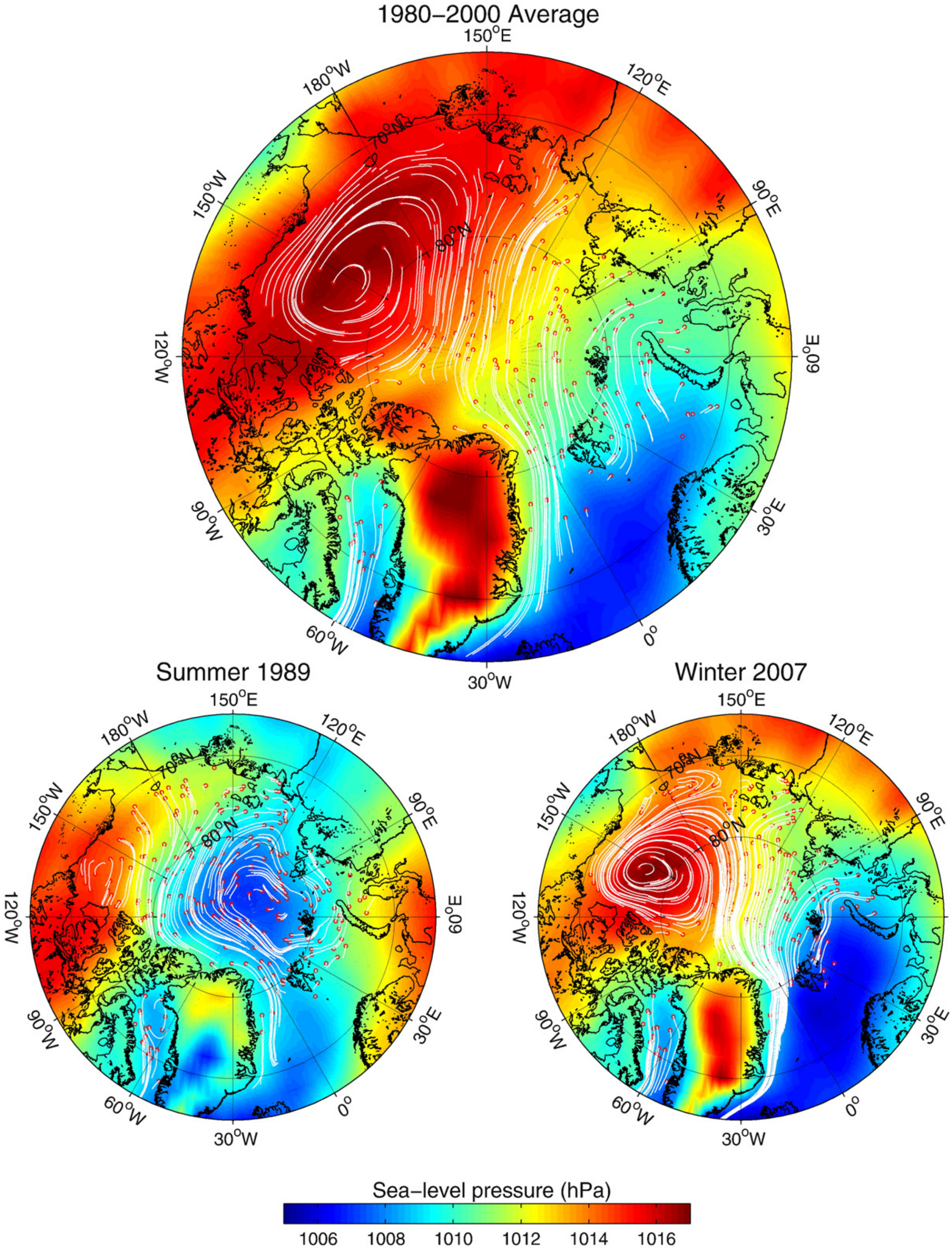

Fig. 5. Atmospheric drivers of Arctic freshwater variability. Each panel shows sea-level pressure (colors; hPa) from the NCEP/NCAR reanalysis product (Kalnay et al., 1996) for the periods indicated. The white lines show the surface flow moving with the average sea ice velocity (from the Polar Pathfinder Sea Ice Motion dataset; Fowler et al., 2013). The small red circles show the starting points for the sea ice trajectories which last two years.

and Ermold, 2004; Dmitrenko et al., 2008). Eurasian runoff is prevented from entering the Canada Basin and exits directly via Fram Strait instead. At these times, Pacific freshwater tends to be incorporated into the Beaufort Gyre and Canada Basin and, subsequently reduces the Pacific contribution to Fram Strait export (Falck et al., 2005; Dodd et al., 2012). The pathway for North American runoff varies; either exiting through the CAA, or entering the Beaufort Gyre (Yamamoto-Kawai et al., 2009). This regime is represented in Fig. 5 by the conditions of winter 2007 (right panel).

This evidence suggests that the Arctic Oscillation and Beaufort High are sometimes linked, sometimes distinct, atmospheric modes that control inter-annual variability in the freshwater system (Morison et al.,

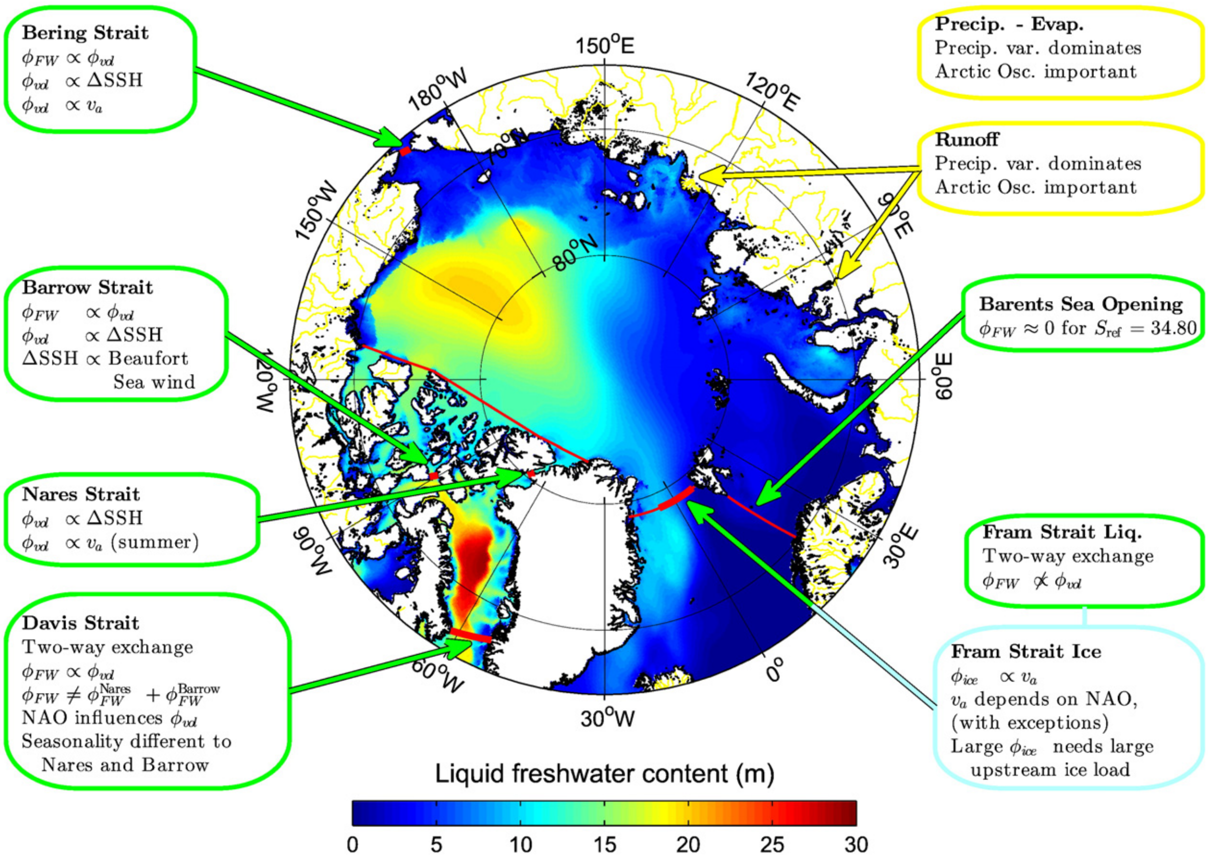

Fig. 6. Mechanisms of Arctic freshwater fluxes discussed in Sections 3.2 and 3.3. ϕ_{FW} is the freshwater flux, ϕ_{vol} is the volume flux, ϕ_{ice} is the ice flux (positive fluxes are poleward), ΔSSH is the sea-level difference (for example between the Bering Sea and the Chukchi Sea in the case of Bering Strait), and v_a is the along-strait component of the surface atmospheric wind (positive poleward). NAO means North Atlantic Oscillation. The proportionality sign means that fluctuations in the two quantities are highly correlated. Colors show the liquid freshwater content (meters, see Eq. (1)) from the PHC 3.0 climatology (Steele et al., 2001) representing, nominally, the period 1980–2000.

2012; Mauritzen, 2012). The wind interacts with the sea ice cover to drive the surface circulation. The surface circulation redistributes freshwater by changing its pathways and residence times. For example, over the period 2005–2008 the Canadian Basin accumulated freshwater while a compensating freshwater loss occurred in the Eurasian Basin (Section 2.2, Morison et al., 2012). Evidently, the Arctic Oscillation determines the freshwater source (runoff, melt) and delivery to the Canadian Basin while the Beaufort High determines Beaufort Gyre freshwater storage. Consistent with these ideas, accumulation of freshwater during the 2000s coincides with increased anti-cyclonic wind over the western Arctic (Proshutinsky et al., 2009; Rabe et al., 2014, Section 2.2, Fig. 5 right panel). The western Arctic can clearly accumulate or release freshwater according to the Beaufort High strength independent of changes in freshwater sources (Stewart and Haine, 2013).

It is also true that changes in the sea ice characteristics may change surface circulation and hence affect freshwater accumulation. For instance, Giles et al. (2012) argue that the increased freshwater seen between 1995 and 2010 (Section 2.2) is because looser sea ice allowed a more efficient momentum transfer from the wind to the ocean, not from more anticyclonic winds. This mechanism may become more important in the future as the summer ice cover disappears.

3.2. Import

Clearly, changes to the long-term (decadal) Arctic Ocean freshwater inventory involve fluctuations in freshwater sources and sinks, not just the wind. We turn to mechanisms controlling sources and sinks of freshwater next. Fig. 6 provides a schematic summary.

3.2.1. Bering Strait

Inter-annual variability in freshwater import to the Arctic through Bering Strait matches or exceeds variability from other sources (Woodgate et al., 2012). For example, the standard deviations of the 2000–2010 annual mean freshwater fluxes shown in Fig. 4 are 200, 270, and 270 $km^3\ yr^{-1}$ for P − E, runoff, and Bering Strait inflow, respectively. This estimate for Bering Strait variability is probably biased low, however, because it derives from changes in the lower layer only and neglects variability in the surface-intensified Alaskan Coastal Current and in the water column stratification (Woodgate et al., 2012).

Mooring measurements show that Bering Strait freshwater variability is strongly correlated with volume-flux variability. Volume-flux changes explain more than 90% of the freshwater-flux changes. In turn, volume-flux changes are related to both changes in the local wind (about 1/3 of the volume-flux variability) and changes in the far-field forcing of the flow (about 2/3 of the variability). The latter is often related to a sea-level difference between the Pacific and the Arctic (Woodgate et al., 2012; references in Woodgate et al., 2005), which in turn is often attributed to a net atmospheric flux of freshwater from the Atlantic to the (fresher) Pacific Ocean (Stigebrandt, 1984).

3.2.2. Runoff and precipitation minus evaporation

The inter-annual changes in runoff to the Arctic and in P − E are controlled by the polar troposphere. Both freshwater sources are ultimately related to the atmospheric moisture flux convergence across the domain boundaries. For variability on inter-annual periods and longer, the effects of water storage in land ice, snow, and watersheds are relatively minor. Thus, variability in atmospheric supply of moisture and hence precipitation control water supply variability to the Arctic Ocean. In general, positive phases of the Arctic Oscillation correspond to greater precipitation in the Arctic and sub-Arctic (Serreze et al., 2008). For example, Peterson et al. (2006) document how positive anomalies in Arctic P − E became more frequent as the NAO changed from mainly negative in the mid-1960s to positive in the early 1990s. Nevertheless, the links between runoff, P − E, and the Arctic Oscillation are not straightforward and other large sources of variability exist. For instance, summer-time convective precipitation over land has little to do with the Arctic Oscillation.

3.3. Export

Now consider mechanisms affecting the export fluxes of freshwater from the CAA through Davis and Fram straits. We discuss the individual channels in the CAA because mechanisms controlling them are better understood than mechanisms controlling the net flux at Davis Strait.[14]

3.3.1. Canadian Arctic Archipelago

Arctic freshwater export through the CAA to Baffin Bay occurs by three main routes; via Barrow Strait to Lancaster Sound, via Nares Strait to Smith Sound, and via Cardigan Strait and Hell Gate (which is narrower) to Jones Sound (Fig. 1). The volume flux through Cardigan Strait is less than half that through Nares or Barrow straits and the freshwater flux is still unobserved (Melling et al., 2008). For this reason we omit Cardigan Strait from the discussion.

3.3.1.1. Barrow Strait. Since 1998 a current meter array has been deployed in Barrow Strait west of Lancaster Sound. The net volume flux is eastward and concentrates at the southern side of the channel. The volume flux is highly variable, with variations as large as the long-term mean of 0.7 Sv (22×10^3 km^3 yr^{-1}). It is stronger in spring and summer than in autumn and winter, perhaps due to land fast ice in winter which retards the surface flow (Prinsenberg and Hamilton, 2005; Melling et al., 2008). The long-term mean freshwater flux is 1500 km^3 yr^{-1} (Prinsenberg and Hamilton, 2005; Prinsenberg et al., 2009; Peterson et al., 2012) accounting for over half of the total Arctic export through the CAA (Beszczynska-Möller et al., 2011).

The freshwater flux at Barrow Strait is highly correlated with the volume flux (the correlation coefficient exceeds 0.96; Prinsenberg et al., 2009); high-resolution numerical models concur (Jahn et al., 2012; McGeehan and Maslowski, 2012). Volume flux is highly correlated with wind conditions in the Beaufort Sea, the latter determining the along-channel sea level difference (the correlation coefficient exceeds 0.80; Prinsenberg et al., 2009). In particular, Peterson et al. (2012) show that northeastward winds in the Beaufort Sea, parallel to the CAA coast, drive the sea-level difference, and hence the volume transport through Barrow Strait. Melling et al. (2008) show that the positive phase of the NAO (and hence the Arctic Oscillation) correlates well with increased freshwater flux at Lancaster Sound with an 8-month delay. These authors suggest that 8 months is the timescale for the Beaufort High to respond to the NAO, weaken the Beaufort Gyre and raise sea level upstream of Barrow Strait.

3.3.1.2. Nares Strait. Volume and freshwater flux observations in Nares Strait are limited, challenging to acquire, and the flow structure is complicated (Münchow et al., 2006, 2007; Melling et al., 2008). Although occasional and short term current observations were made in the 1960s and 1970s (Day, 1968; Sadler, 1976), Nares Strait was the last Arctic gateway where an extensive current meter array was deployed, and not without hardship.[15] The current observations, both from the ship and the moorings, indicate a volume flux at Kennedy Channel (North of Smith Sound) for early August 2003 of about 0.7 Sv (22×10^3 km^3 yr^{-1}) towards Baffin Bay (Melling et al., 2008). A more recent geostrophic estimate is lower, namely, 0.47 ± 0.05 Sv ($15 \pm 2.8 \times 10^3$ km^3 yr^{-1}) (Rabe et al., 2012), but it is an average over 2003–2006 and excludes the contribution from the upper 35 m, where the strongest flow is expected.[16] The freshwater flux through Nares Strait, 890 km^3 yr^{-1} (Rabe et al., 2012), is smaller than that in Lancaster Sound because the Nares Strait outflow is saltier (it carries more Atlantic water; Section 2.5). These measurements suggest that Nares Strait provides 30–50% of the total CAA volume flux and a similar fraction of the total freshwater flux (Beszczynska-Möller et al., 2011).

Nares Strait freshwater flux is driven by the along-channel pressure difference (Münchow and Melling, 2008; also seen in the model of McGeehan and Maslowski, 2012). In summer when the ice is mobile, the along-channel wind is also important in driving the freshwater flux (Rabe et al., 2012). The freshwater flux is influenced by the state of the sea ice, which is either mobile (in summer) or land fast (Samleson et al., 2006; Kwok et al., 2007). With mobile ice the freshwater flux is 20% larger than for land fast ice conditions.

3.3.2. Davis Strait

Arctic water exported through Baffin Bay ultimately transits Davis Strait before entering the Labrador Sea and leaving our control volume. The freshwater flux at Davis Strait does not simply equal the summed CAA fluxes, however. It includes contributions from sea ice processes (freeze/melt); glacial and river runoff; precipitation less evaporation; and contributions from the West Greenland Current. The West Greenland Current enters Baffin Bay at the eastern side of Davis Strait along the West Greenland shelf, flows cyclonically around Baffin Bay to merge with CAA outflows, and exits the western side of Davis Strait as the Baffin Island Current. The West Greenland Current salinity is less than the reference salinity $S_{\mathrm{ref}} = 34.8$ so it adds freshwater to Baffin Bay relative to S_{ref} (Curry et al., 2014). Some of this freshwater was earlier exported from the Arctic through Fram Strait in the East Greenland Current and re-enters the control volume at Davis Strait. Freshwater processes along the path of the East Greenland Current, such as east Greenland runoff and sea ice melt, influence the freshwater content of the West Greenland Current. The net flux across Davis Strait sums these sources of freshwater. As there are several sources to sum there are several mechanisms at work and no single mechanism dominates, unlike in Barrow and Nares straits (see above). Moreover, the relative importance of each contributing mechanism depends on the choice of reference salinity S_{ref} (see Footnote 5).

Some facts hint at the mechanisms controlling the net freshwater flux at Davis Strait, however. First, most of the freshwater flux through Davis Strait comes from the near-surface outflow driven by the CAA inflows to Baffin Bay and the West Greenland Current (Curry et al., 2014, their Fig. 9). Second, observations of the near-surface outflow indicate that freshwater and volume fluxes peak between August and December (Curry et al., 2014). Barrow Strait has peaks in July and August, with minima in November and December (Peterson et al., 2012, their Fig. 4a). Nares Strait freshwater flux is greatest when the sea ice is mobile, rather than land fast in late winter and spring (Rabe et al., 2012). Finally, high-resolution modeling indicates that the freshwater and

[14] Melling et al. (2008) and Beszczynska-Möller et al. (2011) discuss observations of freshwater flux in the CAA.

[15] The array, comprising 16 moorings, was deployed in 2003 from USCGC *Healy* in a joint US–Canadian experiment and was planned to be retrieved from the ice in spring 2005. Due to a severe storm the recovery ice camp had to be abandoned the same day it was established and the retrieval was postponed for a year (Melling, 2011).

[16] The mooring deployments neglect the upper ~30 m to avoid instrument damage by ice keels (Münchow et al., 2006; Rabe et al., 2012).

volume fluxes at Davis Strait are less well-correlated than at Barrow Strait (McGeehan and Maslowski, 2012). This finding suggests that CAA freshwater and volume anomalies de-couple in Baffin Bay and/or that other freshwater sources vary significantly too, disrupting the CAA correlation. Better understanding is needed of how flux variations at Davis Strait inherit from the CAA and the West Greenland Current.

3.3.3. Fram Strait

Fram Strait supports flow in both directions. To the west is the East Greenland Current which carries virtually the entire Arctic sea ice export (Kwok, 2009). To the east the West Spitsbergen Current supplies warm salty water of Atlantic origin to the Arctic, one of the primary Atlantic inflow branches (Section 2.4.3). The net freshwater flux at Fram Strait sums these sources.

Observations show strong correlation between sea ice flux through Fram Strait, which shows large intra- and inter-annual variability, and the cross-strait air pressure difference, which is a proxy for through-strait southward wind (Vinje, 2001; Kwok et al., 2004). The through-strait wind in turn relates to the large-scale atmospheric circulation, in particular the NAO (Köberle and Gerdes, 2003; Kwok et al., 2004). Positive NAO phases correspond to strong Fram Strait winds and thus high sea ice export flux. During times of negative NAO the sea ice flux can be either above or below normal. The flux is high when the Transpolar Drift strengthens and directs ice towards and through Fram Strait (Kwok and Rothrock, 1999; Rigor et al., 2002; Nghiem et al., 2007; Sections 3.1.2, 3.5). Large sea ice export events require a preconditioning of the upstream sea ice field by the large-scale atmospheric circulation, followed by favorable wind conditions local to the Fram Strait (Kwok, 2009). In the last decade it appears that cross-strait air pressure difference increased while sea ice concentration decreased (Kwok, 2009).

The mechanisms governing the Fram Strait liquid freshwater flux are poorly known. Liquid freshwater is exported through the western end of Fram Strait over the Greenland shelf and shelf break within the East Greenland Current (between 3° and 8°W; de Steur et al., 2009; Rabe et al., 2013). The interaction and exchange with the warm salty West Spitsbergen Current to the east is hard to observe and not well understood. Observations show that the freshwater and volume fluxes exhibit large inter-annual variability (visible in Fig. 4). A seasonal cycle also exists with flux peaks in September and March (Jahn et al., 2010; Dodd et al., 2012). During winter the East Greenland Current is mainly barotropic: in summer there is also a baroclinic component (Aagaard and Coachman, 1968). Fluctuations in both outflow salinity and speed apparently influence freshwater flux anomalies based on Jahn et al.'s (2012) analysis of eight model hindcasts for the last 20–60 years. Unlike the CAA, the correlation between freshwater and volume flux through Fram Strait is weak, however. At times of large liquid freshwater export the halocline deepens over the Greenland shelf in the western Fram Strait and the front with the West Spitsbergen Current steepens (Rabe et al., 2013; Köberle and Gerdes, 2007).

3.4. Rotational export control model

We now discuss controls on freshwater outflow due to rotational dynamics, which are relevant to the Arctic straits. Rotational controls lead to a simple model of freshwater export fluxes. The model flux results are compared to the observed fluxes from Section 2 (Fig. 4) and provide a context for interpreting the predictions of climate models discussed in Section 4 (Fig. 9).

Arctic outflow through an opening wider than the first baroclinic Rossby radius is affected by the Earth's rotation (Jakobsson et al., 2007). In these cases, the outflowing layer adheres to the right of the strait (Werenskiold, 1935). The outflow of the East Greenland Current through Fram Strait was described this way by Wadhams et al. (1979). Similarly, Stigebrandt (1981) used rotational control in a two-layer model of Arctic outflow. Later elaborations by Björk (1989) and Rudels (1989) introduced water mass formation processes on the shelves and Hunkins and Whitehead (1992) studied Fram Strait exchanges with a laboratory experiment. Rotational controlled outflows have recently been studied by Nilsson and Walin (2010) and Rudels (2010).

Salinity controls stratification in the upper Arctic Ocean, and the Rossby radius is determined by the freshwater export flux, lower layer salinity, and Coriolis parameter. The Rossby radius is independent of the mixing rate and volume flux in the upper layer (Rudels, 2010). This means that the Rossby radius is controlled by the freshwater thickness at the strait, m_s (see Eq. (1) in Footnote 1), not by the total depth of the upper layer. The freshwater export flux through the channel is proportional to m_s^2. If one assumes that m_s equals the average value of m (the liquid freshwater content; Eq. (1)) over the Arctic, then the export flux is related to the storage of freshwater in the Arctic Ocean interior. Then, if the total freshwater export flux is known, or can be estimated, it is possible to estimate the freshwater storage, and vice versa (Rudels, 2010).

Barrow, Nares, and Fram straits are wide enough to support a rotational outflow in the upper layer of this type. By taking the lower layer salinities and the upper layer depths to be equal in these passages, Rudels (2010) estimated the mean thickness of the freshwater layer in the interior Arctic Ocean to be about 8 m. In the absence of ice export, the freshwater storage must increase to more than 10 m to maintain a freshwater balance (Rudels, 2010). The average liquid freshwater thickness over the Arctic Ocean is 8 m, in good agreement.[17] The assumption of equal salinity in the lower layers in all three straits is unrealistic. The deep salinity in Fram Strait is about 35, but in the CAA it is 33.5–34. Nevertheless, this discrepancy is compensated by a fresher upper outflow through the CAA than through Fram Strait so that the differences in densities between the upper and lower layers in each passage are similar.

Davis Strait is also wide enough to support rotational outflow and a two-way exchange between Baffin Bay and the Labrador Sea (Section 3.3.2). Rudels (1986) and Rudels (2011) estimated these fluxes using geostrophic balance. To obtain unique solutions he made assumptions about ice formation in Baffin Bay (Rudels, 1986) or applied a sea-level difference between the Lincoln Sea and the Labrador Sea that drives the deep outflow through Davis Strait (Rudels, 2011). Two effects appeared in this model. First, freshwater input to Baffin Bay (directly or through Davis Strait) freshens the upper layer in Baffin Bay and can reduce volume flux entering through the CAA. The fresh Arctic Ocean upper layer exits the Arctic Ocean through Fram Strait instead. It may eventually arrive in Baffin Bay via the West Greenland Current, thus further freshening the upper layer and reducing the CAA outflow. Second, the Lincoln Sea/Labrador Sea sea-level difference also drives a rotational flow through the passages, but was not considered. For this reason the Rudels (2011) estimate of the Arctic Ocean freshwater storage is likely too high.

It is instructive to apply this idealized rotational export model to the flux time series shown in Fig. 4. As above, we assume that at Davis and Fram straits the freshwater thickness m_s equals $\overline{m}$, the average value of the freshwater thickness m over the domain. The freshwater budget is:

$$A\frac{\mathrm{d}\overline{m}}{\mathrm{d}t} = F_{\mathrm{in}}(t) + \mathcal{M}(t) - \alpha A^2\overline{m}^2, \tag{2}$$

$$\frac{\mathrm{d}I}{\mathrm{d}t} = F_{\mathrm{ice}}(t) - \mathcal{M}(t). \tag{3}$$

Here, A is the area of the domain (including the CAA and Baffin Bay), F_{in} is the total inflowing freshwater flux, $\mathcal{M}$ is the freshwater flux due to

[17] The area of the region is 9.7×10^6 km^2 (Section 3.1.1) and the 1980–2010 average liquid freshwater volume is 97,000 km^3 (Table 1).

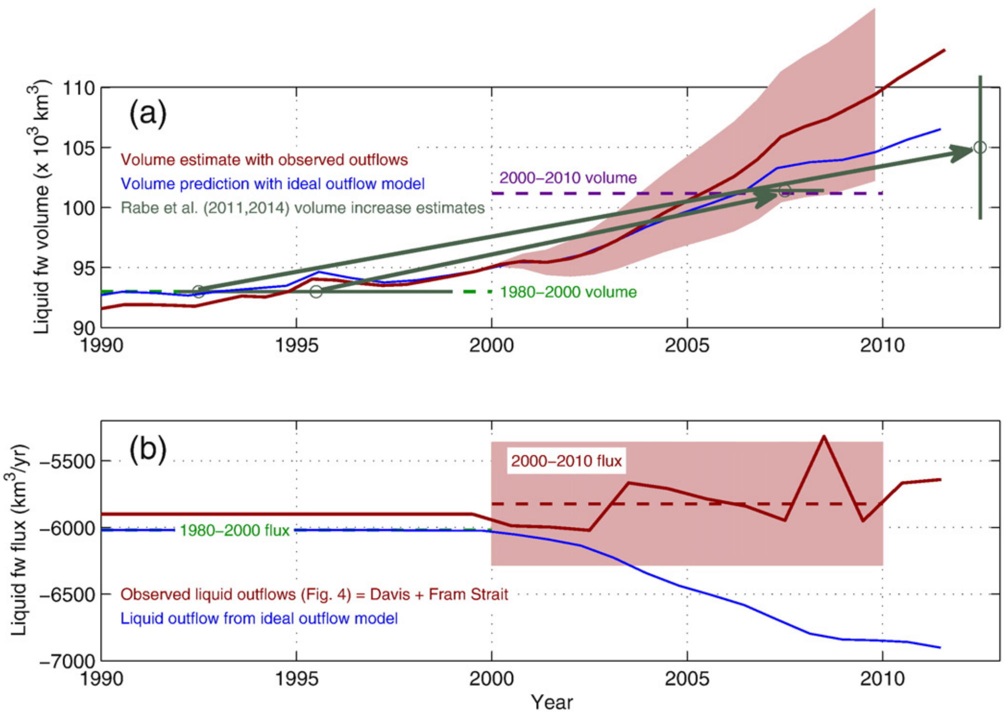

Fig. 7. Idealized outflow model predictions of liquid freshwater (fw) (a) volume (for the Arctic, CAA, and Baffin Bay), and (b) export flux (through Davis and Fram straits). The blue lines show the predictions of the idealized liquid export flux model (see Eq. (2) in Section 3.4). The red lines show the observed liquid export fluxes (in (b)) and the volume estimate from the integral of the net flux (in (a); see text). The shading indicates the uncertainty in the 2000–2010 average liquid export flux (in (b)), and the corresponding accumulated volume uncertainty (in (a)). Dashed lines show average freshwater volume and export fluxes. Arrows show the estimates of Rabe et al. (2011) and Rabe et al. (2014) (Section 2.2).

melting ice, and α is the proportionality coefficient between flux and m_s.[18] Also, I is the volume of freshwater stored in ice and $F_{\rm ice}$ is the export ice flux through Fram Strait (which is negative leaving the Arctic as in Fig. 3; we neglect any inflow of ice). We have estimates of $I(t)$, $F_{\rm in}(t)$, and $F_{\rm ice}(t)$ from Figs. 3 to 4 for the last two decades ($F_{\rm in}$ is the sum of the runoff, P − E, and Bering Strait inflows). Using them we integrate Eq. (2) starting in 1990. Fig. 7 shows the results for the time-varying freshwater volume, $A\overline{m}$, and the total liquid export flux, $\alpha A^2 \overline{m}^2$. The figure also shows the sum of the observed liquid freshwater fluxes through Davis and Fram straits from Fig. 4. Finally, it shows the corresponding liquid freshwater volume obtained by integrating the net flux convergence (that is, by replacing the final term in (2) with the observed export flux; the red line in Fig. 7b). The observed fluxes imply convergence of freshwater in the 2000s. The implied freshwater accumulation is similar to, but somewhat greater than, the independent accumulation estimates of Rabe et al. (2011) and Rabe et al. (2014). They consider only the Arctic Ocean with a bottom depth deeper than 500 m, however, which is smaller than our domain (see Section 2). The average for the period 2000–2010 is 101,000 km^3, the value quoted in Table 1 and Section 2.

The idealized outflow model (2) predicts an increasing export flux in the 2000s and hence a smaller increase in liquid freshwater volume. These changes were not observed. A simple explanation for the difference between the predictions of the idealized outflow model and the observed freshwater volumes and fluxes is that the freshwater thickness at Davis and Fram straits did not increase. In other words, m_s was unchanged and was not proportional to $\overline{m}$ in the 2000s. The wind sequestered the extra freshwater in the Beaufort Gyre, away from the drainage channels (as discussed in Sections 2.2 and 3.1.2).

Finally, the idealized outflow model connects the export flux to the freshwater thickness squared. This nonlinearity is unimportant in practice, however, because the volume fluctuations are relatively small. Solutions of Eq. (2) therefore show nearly exponential relaxation with characteristic timescale $1/(\alpha V_{\rm avg}) \approx 15$ yr, where $V_{\rm avg}$ is the average liquid freshwater volume for 1980–2000 (taken as 93,000 km^3 from Table 1). This relaxation period is the timescale needed to restore balance between freshwater input and export. It is about ten times longer than the timescales over which the wind modifies the export fluxes through the different channels (Stewart and Haine, 2013).

3.5. Historical freshwater export events: Great Salinity Anomalies

What can we learn about freshwater mechanisms from the historical record of variability? Perhaps the most remarkable example of a large freshwater variation is the Great Salinity Anomaly (GSA) of the late 1960s and 1970s. This event was a propagating, decadal-scale, surface-intensified freshening of the subpolar North Atlantic and Nordic Seas (Dickson et al., 1988). It has been attributed to Arctic freshwater export anomalies of about 10,000 km^3 over 5 years (Curry and Mauritzen, 2005). Two similar events have been observed: in the 1980s (Belkin et al., 1998), and 1990s (Belkin, 2004). Others may have gone unobserved (Wadley and Bigg, 2004). Indeed, time series of salinity in the North Atlantic reveal several smaller anomalies (Sundby and Drinkwater, 2007), and by "GSA" we refer collectively to the 1970s GSA and other GSA-like events. On reaching the Labrador Sea, GSAs apparently follow similar cyclonic paths around the subpolar North Atlantic and Nordic Seas. The 1970s, 1980s, and 1990s anomalies are detectable in salinity data for about a decade.

A link may exist between GSAs and the large-scale wind circulation regime, especially the NAO, although it is not well understood (Dickson et al., 2000). Cyclonic winds over the Canada Basin tend to increase freshwater export from the Arctic and anticyclonic winds tend to retain freshwater there (Section 3.1.2). The 1980s and 1990s events occurred when the winds were cyclonic and both of these anomalies apparently emerged west of Greenland. The 1970s GSA occurred when the winds

[18] $\alpha = 7 \times 10^{-7}$ km^{-3} yr^{-1} and ensures balance on average over the period 1980–2000 between $F_{\rm in}$, $\mathcal{M} = F_{\rm ice}$, and the outflowing liquid freshwater flux.

were strongly anticyclonic, however, suggesting that freshwater should have been strongly retained in the western Arctic. This "paradox" (Dickson et al., 2000) can be understood by recalling that the Transpolar Drift strengthens under anticyclonic wind forcing (as in 2007; Fig. 5 lower right panel). Fram Strait freshwater export can increase at these times (mainly due to the export of sea ice) even as Beaufort Gyre freshwater content rises. Hence, a GSA during cyclonic (anticyclonic) winds likely results from an increased liquid freshwater export through the CAA (increased sea ice export through Fram Strait). Recent work suggests that a large wind-driven freshwater release, around 10,000 km^3 in 5 years, can only occur if freshwater storage in the Beaufort Gyre is already anomalously high (Stewart and Haine, 2013). Otherwise, the freshwater volume released is significantly smaller.

The mechanism of GSA propagation is an open question. Specifically, the decadal lifetime is hard to understand. One idea is that anomalous packets of freshwater are advected passively by the otherwise unchanged currents (Belkin et al., 1998). Numerical models of GSA propagation implicate freshwater flux anomalies and/or circulation anomalies, however (Wadley and Bigg, 2006). Time series observations reported by Sundby and Drinkwater (2007) seem to agree. A positive feedback may be important: the fresh surface damps deep convection, reducing both sea-surface temperature and ocean–atmosphere heat flux (Gelderloos et al., 2012). This cooling favors precipitation, further reinforcing the fresh anomaly.

3.6. Summary of freshwater mechanisms

The main points are summarized as follows (see the cited sections and figures for details):

- The Arctic upper Ocean is relatively fresh because it has a large supply of freshwater from runoff, Bering Strait inflow, and precipitation compared to its volume. Seasonal freezing and melting promote a fresh surface by ice distillation. Also, the turbulence intensities in the halocline are exceptionally small, reducing the flux of salt mixed up from below (Section 3.1.1).
- Wind stress over the Arctic controls ice motion and the surface ocean currents, and hence determines freshwater pathways and accumulation (Section 3.1.2; Fig. 5). The Arctic Oscillation and fluctuations in the atmospheric Beaufort High sea-level pressure are particularly influential. In the last decade there has been an increase in Ekman pumping driven by the Beaufort High that has increased freshwater storage in the Beaufort Gyre at least partly by drawing freshwater from other regions.
- Convergence of tropospheric moisture, and hence precipitation, controls the net supply of freshwater to the Arctic from the atmosphere (Section 3.2.2). The Arctic Oscillation is an important, but not dominant, influence on this mechanism.
- The marine freshwater inflow through Bering Strait is believed to be controlled by the Pacific-to-Arctic sea level difference and moderated by the local southward wind (Section 3.2.1, Fig. 6). In Bering Strait the fluctuations in volume flux are highly correlated with those in freshwater flux.
- Similarly, fluctuations in volume flux and freshwater flux are highly correlated in Barrow and Nares straits (Section 3.3.1). In both these channels the volume flux is highly correlated with the along-channel sea level difference. In Barrow Strait the along-channel sea level difference correlates with the Beaufort Sea wind field. In Nares Strait the along-channel southward wind correlates with the volume and freshwater fluxes in summer when the ice is mobile.
- Davis and Fram straits support two-way exchange and several mechanisms compete because there are several sources of freshwater contributing to the net flux through these straits (Sections 3.3.2 and 3.3.3). Fram Strait ice flux is driven mainly by the local southward wind. Sea ice decline in the 2000s is apparently compensated by increased flow speed to maintain about the same sea ice flux through Fram Strait.
- An idealized model of a rotational outflow predicts that the liquid freshwater flux is controlled by the liquid freshwater content at the export straits (Section 3.4). The characteristic response timescale of the model is 15 years. Over the 2000s, the model predicts an increasing outflow through Davis and Fram straits (Fig. 7). The observed freshwater fluxes did not change significantly, however, because the excess freshwater was stored in the Beaufort Gyre away from the drainage channels. The observed fluxes (Fig. 4), and loss of sea ice (Fig. 3), suggest accumulation of liquid freshwater that is consistent with observations, although the uncertainties are large (Fig. 7).
- Three major freshwater export events seem to have occurred since the mid-1960s; two through the CAA and Baffin Bay, and one through Fram Strait (Section 3.5). They caused Great Salinity Anomalies that moved through the subpolar North Atlantic and Nordic Seas in about ten years. The export mechanism apparently involves wind shifts in the Beaufort Sea, but the details are not understood. The mechanism behind the long lifetime is also unknown.

To conclude this section on freshwater mechanisms, the importance of unforced, internal variability should not be forgotten. By unforced variability we mean fluctuations that are not due to changes in forcing from the atmosphere or due to changes in sources and sinks of freshwater. Instead, the variability is caused by intrinsic chaotic dynamical processes in the ocean/ice system. It is hard to quantify the magnitude of such variability, but for the total freshwater volume it appears to be several thousand km^3 based in Arctic/sub-Arctic Ocean/ice models with steady forcing (Stewart and Haine, 2013). Almost certainly, the decline in sea ice since 2000 is due to anthropogenic climate change, not internal variability (Notz and Marotzke, 2012), but the contribution of natural variability to changes in the freshwater reservoir volume is unclear. The forcing and supply mechanisms identified in this section compete with these unforced internal fluctuations and are often hard to distinguish.

4. Prospects for Arctic freshwater

Climate model projections of Arctic freshwater variables are diverse and thus uncertain. Nevertheless, most climate model projections of Arctic freshwater variables are similar enough to infer some probable changes in the future Arctic liquid freshwater storage and export. Here we discuss these prospects and compare the freshwater changes described in Section 2 with climate model projections. The overarching question is: How do we expect the freshwater system will change in the future?

4.1. Robust climate signals

There are several robust signals that emerge consistently from climate model projections: First, a warmer climate features a stronger hydrological cycle with greater atmospheric moisture transport to high latitudes. Therefore, precipitation over, and runoff to, the Arctic Ocean is projected to increase based on coupled climate models (see Kattsov et al. (2007), for an overview of CMIP3[19] models and Vavrus et al. (2012), for an example of a CMIP5 model). For example, the Community Climate System Model, version 4 (CCSM4) shows about a 40% increase in precipitation polewards of 70°N over the 21st century (Vavrus et al., 2012). The main reason Arctic precipitation increases in CMIP5 models is increased local evaporation (in winter), signifying an accelerated freshwater cycle within the Arctic itself (Bintanja and Selten, 2014). Increased atmospheric moisture transport is less important

[19] CMIP is the Coupled Model Intercomparison Project serving coupled climate model projections to the Intergovernmental Panel on Climate Change (IPCC). CMIP3(5) models are from the fourth (fifth) assessment reports in 2007 (2013).

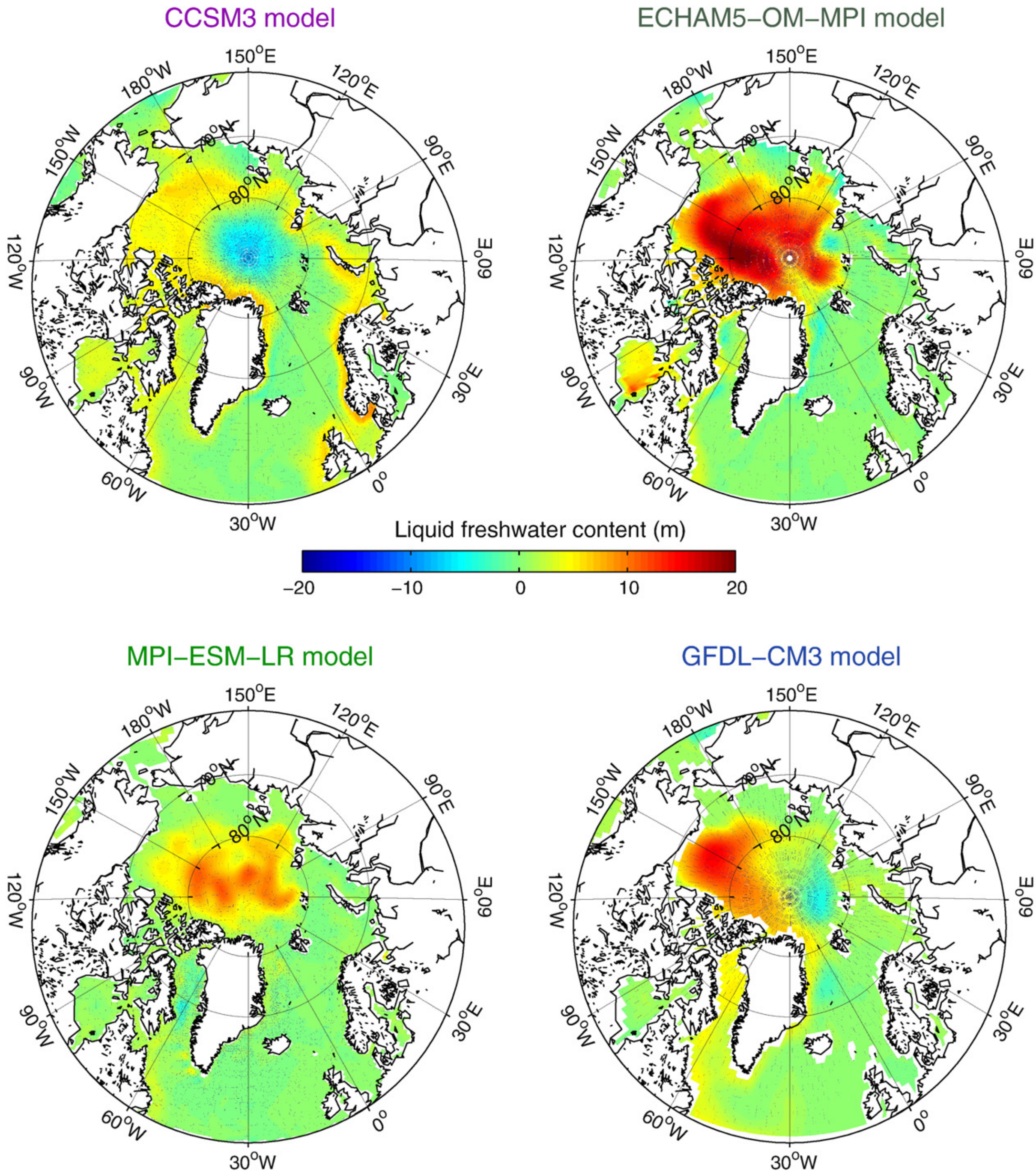

Fig. 8. Arctic Ocean liquid freshwater content differences between the end (2090–2100 average) and the beginning (2000–2010 for the upper panels, 2010–2020 for the lower panels) of the 21st century from four CMIP climate models. Upper panels show two CMIP3 models (A1B scenarios; CCSM3 and ECHAM5-OM-MPI). Lower panels show two CMIP5 models (RCP4.5 scenarios; MPI-ESM-LR and GFDL-CM3).

(and peaks in late summer and autumn). Second, sea ice extent declines in the northern hemisphere in all seasons (IPCC (2007), Chapter 10). The rate of decline differs greatly among models and most models underestimate the recently-observed summer sea ice retreat seen in Fig. 3 (Section 2.3). The aforementioned acceleration in Arctic precipitation and evaporation is linked to winter-time sea-ice retreat (Bintanja and Selten, 2014). Third, ice volume decreases in all CMIP5 models over the 21st century (Julienne Stroeve, pers. comm., 2012). The volume of sea ice at the end of the 20th century and the rate of change in Arctic sea ice volume again vary greatly among models. The declining ice volume results in smaller ice thickness in Fram Strait and decreasing ice export rates (Holland et al., 2007; Koenigh et al., 2007; Vavrus et al., 2012). Because both sea ice volume and export flux decrease over time, the net (annual-mean) thermodynamic growth rate must also decline. It is possible, however, that the seasonal cycle might increase with higher freezing and melting rates in the Arctic Ocean.

4.2. Consequences for freshwater storage and export

Increasing freshwater input into the Arctic Ocean through P − E and runoff and decreasing ice export flux implies either (transient) liquid freshwater storage or increasing liquid freshwater export rates from the Arctic (or both). Different models behave differently in these respects. For example, the freshwater content changes over the 21st

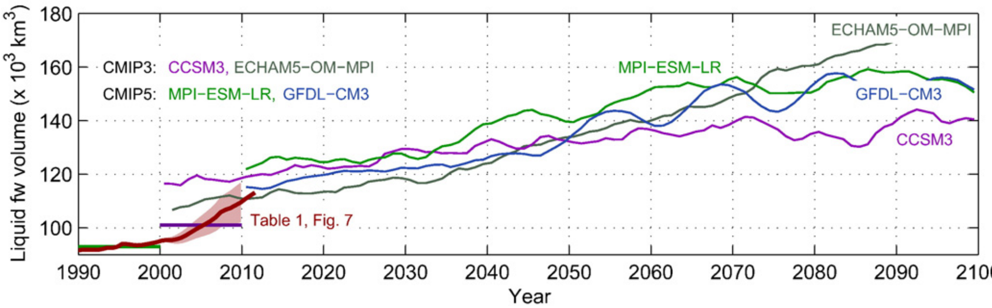

Fig. 9. Twenty-first century liquid freshwater (fw) prospects from CMIP models. The volume of liquid freshwater for the Arctic Ocean, CAA, and Baffin Bay is shown. The estimates from Table 1 and Fig. 7 are shown at the bottom left. The CMIP3 (CMIP5) models are realizations of the A1B (RCP4.5) scenario.

century are shown for four CMIP models in Fig. 8. The upper panels show the differences in liquid freshwater content between the end (2090–2100 average) and the beginning (2000–2010 average) of the 21st centuries for the CCSM3 and ECHAM5-OM-MPI models (both from CMIP3). Only one realization of the IPCC's A1B scenario is shown although the decadal variability can be substantial. We see gains of several meters in CCSM3 in the western Arctic whereas the eastern Arctic loses freshwater (compare to Fig. 6). In the ECHAM5-OM-MPI model, freshwater content increases by 10–20 m over virtually the whole Arctic Ocean. The total liquid freshwater content increases by 24,000 km^3 (from 118,000 to 142,000 km^3) in the CCSM3 model over the 21st century. For the ECHAM5-OM-MPI model, the corresponding increase is 63,000 km^3 (from 110,000 to 173,000 km^3). These models begin the 21st century with moderately realistic total liquid freshwater volumes: for the decade of the 2000s the estimate from Section 2 is 101,000 km^3 (Table 1).

A likely reason for these striking freshwater differences is different ocean volume (and freshwater) fluxes between the Arctic and the subpolar North Atlantic. In the ECHAM5-OM-MPI model, increasing meteoric freshwater input and reduced sea ice export lead to increased storage of liquid freshwater. The CCSM3 model responds to these input and ice changes by increasing oceanic volume exchange with the subpolar Atlantic. For example, the surface salinity decreases along the export pathways east and west of Greenland and in the western Labrador Sea (not shown). As a consequence, more saline Atlantic water enters the Arctic, reducing the freshwater content in the eastern Arctic Ocean. The integrated response in Arctic and CAA freshwater storage is smaller in CCSM3 compared to ECHAM5-OM-MPI for these reasons.

Liquid freshwater content differences are shown for two CMIP5 models in the lower panels of Fig. 8 (RCP4.5 scenario). They behave similarly to the CMIP3 calculations with CCSM3 and ECHAM5-OM-MPI. Again, in some places the freshwater content increases, but in others it decreases. The same is true for the surface salinity (not shown). For example, the MPI-ESM-LR model freshens in all deep basins of the Arctic Ocean and increases salinity on most shelves. Enhanced import of saltier Atlantic waters causes salinity to increase below the halocline whereas liquid freshwater content increases in the Beaufort Gyre. The MPI-ESM-LR model accumulates 33,000 km^3 (from 125,000 to 155,000 km^3) liquid freshwater in the 21st century. In contrast, the GFDL-CM3 model accumulates freshwater in the Beaufort Gyre and Lincoln Sea and loses it in the Eurasian Basin; the shelf salinities change only weakly. The GFDL-CM3 model accumulates 36,000 km^3 (from 117,000 to 153,000 km^3) liquid freshwater over the 21st century for this realization.

Vavrus et al. (2012) describe the Arctic Ocean evolution over the 21st century in the CCSM4, the NCAR model used for CMIP5. CCSM4 includes an open Nares Strait, unlike CCSM3, which allows an increased freshwater export through the CAA. Vavrus et al. (2012) find a freshening of the surface in the Arctic Ocean over the 21st century. There is a 28% increase in liquid freshwater storage in the Arctic Ocean. This increase is very similar to those for the MPI-ESM-LR and GFDL-CM3 models, quoted above (although the details of the liquid freshwater content calculations differ: Vavrus et al. (2012) consider only the upper 250 m of the Arctic Ocean and exclude the CAA and Baffin Bay). The CCSM4 sea ice stores 80% less liquid freshwater by the late 21st century. Together, liquid and sea ice account for a moderate increase of 9% in the total freshwater storage. CCSM4 Bering Strait freshwater flux into the Arctic also increases. The liquid freshwater export through Fram Strait increases through the 21st century (by about 3200 km^3 yr^{-1}), whereas sea ice export drops substantially (by about 1800 km^3 yr^{-1} to about 600 km^3 yr^{-1}). The liquid freshwater export through the CAA first increases (by about 900 km^3 yr^{-1}) then decreases after 2070 (by about 300 km^3 yr^{-1}) when decreasing CAA volume flux dominates the decreasing salinity. This development is attributed to weakening convection in the Labrador Sea, which grows fresher over the 21st century. If CCSM4 behaves similarly to CCSM3, the downstream freshening would raise sea level and decrease the surface pressure gradient between the Arctic and the Labrador Sea, hence reducing the CAA volume flux. Details of this mechanism remain unclear, however. Finally, Vavrus et al. (2012) find strongly increasing temperature of the CCSM4 Atlantic Water layer indicating stronger inflow of Atlantic Water.

4.3. Summary of freshwater prospects

Fig. 9 condenses the results from these CMIP climate models. It shows time series over the 21st century of the volume of liquid freshwater, and includes the results of the budget analysis in Section 2 and the freshwater model in Section 3. Given the various sources of error, and variability, we see good agreement in general. The models overestimate the liquid freshwater volume somewhat, but the discrepancy is only 10–20% of the total. The increasing freshwater trend inferred from observations in Fig. 7a (the red line) is similar to, but generally greater than seen in the models. Recall that the models underestimate the decline in ice volume, however, compared to the observations. In other words, the models underestimate the increasing liquid freshwater trend in the first few decades of the 21st century for this reason. Finally, the models show consistent increases in freshwater until at least mid-century. After that, some reductions in freshwater volume of 5000–10,000 km^3 over 5–10 years occur, for the GFDL-CM3 model, in particular. These events may resemble GSAs (Section 3.5), although it is presently unknown if the CMIP climate models can realistically simulate GSAs.

Summarizing:

- The CMIP models consistently predict an increasing hydrological cycle with greater precipitation, evaporation, and runoff, polewards of 70°N by 2100 (Section 4.1; Vavrus et al., 2012; Bintanja and Selten, 2014). Sea ice extent and volume are projected to decrease, with large variability between models (Section 4.1) and loss rates significantly lower than observations. The total liquid freshwater volume is projected to increase by about 50,000 km^3 between 2000 and 2100 (Fig. 9). Liquid freshwater in the Beaufort Gyre will likely also increase, although there is significant variability among models (Fig. 8).
- The best evidence to date on climate projections of marine freshwater fluxes comes from the CCSM4 model (Vavrus et al., 2012). In CCSM4, Bering and Fram Strait liquid freshwater fluxes increase (Section 4.2). The CAA liquid flux increases to 2070 then declines thereafter in this model. Sea ice export through Fram Strait declines substantially through the 21st century.

To conclude this section on freshwater prospects, refer to the final column in Table 1. The prospects for the freshwater budget for the 21st century are quantified where possible based on the CMIP climate models. Each value derives from numbers quoted in Section 4.[20] Ignoring changes in the minor components (which have question marks in Table 1), we anticipate that the sources of freshwater to the Arctic will increase, from about 9400 to perhaps 11,000 $km^3\ yr^{-1}$, by 2100.[21] The sinks of freshwater draining the Arctic will also likely increase, from about 8250 to perhaps 10,000 $km^3\ yr^{-1}$. These numbers indicate that the Arctic freshwater cycle will accelerate in the 21st century with significantly increasing inflow, outflow, and storage of freshwater. It is likely that the freshwater budget in 2100 will not be balanced: the freshwater sources will probably exceed the sinks and the Arctic will continue freshening. These estimates are provisional and uncertain, as discussed above.

5. Conclusions

This paper has reviewed published literature on the status, mechanisms, and prospects for freshwater, and especially freshwater fluxes, in the Arctic and Subarctic Ocean. Where possible, we have synthesized these prior works. The main findings are:

- Freshwater is accumulating in the Arctic, CAA, and Baffin Bay (Section 2.2): about 8000 km^3 more freshwater was present in the decade of the 2000s compared to the 1980–2000 average (Table 1). Accumulation is mainly in the Beaufort Gyre, where the increase was about 5000 km^3.
- Sea ice extent, volume, and age have decreased in the 2000s compared to 1980–2000 (Section 2.3, Fig. 3).
- The meteoric fluxes supplying freshwater (runoff and precipitation) have increased in the 2000s compared to 1980–2000 (Section 2.4, Table 1, Fig. 4; most of the evidence comes from models). Despite flux increases from 2001 to 2011, it is uncertain if the marine freshwater source through Bering Strait for the 2000s has changed, as observations in the 1980s and 1990s are incomplete. The total marine flux draining freshwater (liquid and as ice through Fram and Davis straits) has not changed significantly. The net flux of freshwater has therefore increased, to about $1200 \pm 730 km^3\ yr^{-1}$.
- The observed increase in liquid freshwater storage in the 2000s is consistent with the shift in freshwater fluxes and the loss of freshwater as sea ice, although the uncertainty is large (Fig. 7).
- Understanding of the mechanisms controlling Arctic freshwater fluxes and storage points to the importance of the surface wind field (Sections 3.1.2–3.3, Fig. 6). The wind controls the surface ocean circulation (Fig. 5) and hence freshwater transport rates and pathways (Section 2.5).
- The characteristic timescale for changes in the freshwater system due to source or sink changes is about 15 years (Section 3.4). The timescale for export flux changes driven by the wind is much shorter, perhaps O(1–10) months (Section 3.4). Because the wind controls these changes, they are less predictable than those caused by variability of freshwater sources. Large freshwater export events, Great Salinity Anomalies (GSAs, Section 3.5), have been observed in the last 50 years, probably triggered by changes in the Arctic surface winds.
- Although inherently uncertain, coupled climate models simulate Arctic freshwater processes in several realistic ways (Section 4, Fig. 9). Their predictions for the 21st century show continued acceleration of the hydrological cycle, with roughly an extra 50,000 km^3 liquid freshwater stored by 2100 (Section 4.3, Table 1). Climate models predict that the marine export fluxes of liquid (ice) freshwater will increase (decrease) enough to be detected by the export monitoring arrays. They underestimate the speed of sea ice decline, however. Also, it is unclear if they capture GSA mechanisms, and therefore may be incapable of simulating rapid freshwater discharge events.
- The impacts of these changes in the Arctic freshwater system are diverse. They include effects within the Arctic Ocean, such as albedo and upper-ocean stratification changes, which in turn may affect the heat budget, mineral nutrient supply to phytoplankton, and the light environment near the surface. And they reflect the view that climate change in the Arctic is amplified. A thorough review of these impacts is beyond the current scope, but would be interesting and valuable (for example, see Bhatt et al., 2014 on implications of sea-ice decline).

Future work on Arctic freshwater should continue to focus on the gateway fluxes through straits. Although no significant changes in export fluxes have yet been seen, it is likely they will occur, perhaps suddenly, in response to changes in Arctic wind. Future work should maintain the hydrographic sampling of the Arctic Ocean to determine freshwater storage changes. Chemical tracers are essential too, in order to distinguish different freshwater origins and pathways. The mechanisms discussed in Section 3 are valuable because they provide a basis to test and refine the coupled climate models discussed in Section 4, and discriminate between them. Understanding the freshwater processes in these models is another priority, as is examining their freshwater budgets in detail, for example using the framework of Section 2. Future work to deepen understanding of the mechanisms controlling freshwater accumulation and release will potentially aid in observing strategies. For example, processes controlling sea level are important because sea level differences are linked to volume fluxes and hence freshwater fluxes, especially west of Greenland. Finally, it seems likely that many Arctic freshwater mechanisms will change with the impending loss of summer sea ice. They include some of the processes that maintain the fresh basic state of the upper ocean (Section 3.1.1). Anticipating, observing, and understanding those changes is an unprecedented opportunity that will further elucidate the dynamics of the Arctic freshwater system.

Acknowledgments

The authors are supported by the U.S. National Science Foundation (awards OCI-0904338, ARC-0855748, PLR-1304052, OPP-0230381, and OPP-0632231), the Office of Naval Research (N00014-13-1-0468), the National Oceanic and Atmospheric Administration (RUSALCA program),

[20] To estimate the runoff increase we take Vavrus et al.'s (2012) 40% precipitation increase and reduce it to 30% based on Fig. 1a of Bintanja and Selten (2014), which shows precipitation over land increases less than over the ocean. The P − E increase is estimated as 300 $km^3\ yr^{-1}$ from Bintanja and Selten's (2014) Fig. 2a (inset). The entry for the Greenland flux is based on extrapolating Bamber et al.'s (2012) estimates (see Section 2).

[21] This estimate excludes changes in the Bering Strait inflow, which increases in CCSM4 but has not been quantified (Vavrus et al., 2012).

the Fisheries and Oceans, Canada, the European Union 7th Framework (grant agreements 212546 THOR, 308299 NACLIM, and project ICE-ARC), the ICE Centre at the Norwegian Polar Institute, the Research Council of Norway CORESAT project, and the German Federal Ministry of Education and Research (project RACE — Regional Atlantic Circulation and Global Change, 0F0651 D). We acknowledge the modeling groups, the Program for Climate Model Diagnosis and Intercomparison and the World Climate Research Program's Working Group on Coupled Modeling for their roles in making available the CMIP3 multi-model dataset. Support of this dataset is provided by the Office of Science, U.S. Department of Energy.

References

Aagaard, K., Carmack, E.C., 1989. The role of sea ice and other fresh-water in the Arctic circulation. J. Geophys. Res. 94, 14,485–14,498.

Aagaard, K., Coachman, L.K., 1968. The East Greenland Current north of Denmark Strait: part I. Arctic 21, 181–200.

Alkire, M.B., Falkner, K.K., Rigor, I., Steele, M., Morison, J., 2007. The return of Pacific waters to the upper layers of the central Arctic Ocean. Deep-Sea Res. I 54 (9), 1509–1529. http://dx.doi.org/10.1016/j.dsr.2007.06.004.

Bailey, W.B., 1956. On the origin of deep Baffin Bay water. J. Fish. Res. Board Can. 13, 303–308.

Bamber, J., van den Broeke, M., Ettema, J., Lenaerts, J., Rignot, E., 2012. Recent large increases in freshwater fluxes from Greenland into the North Atlantic. Geophys. Res. Lett. 39, L19501. http://dx.doi.org/10.1029/2012GL052552.

Bauch, D., Schlosser, P., Fairbanks, R.G., 1995. Freshwater balance and the sources of deep and bottom waters in the arctic ocean inferred from the distribution of $H_2^{18}O$. Prog. Oceanogr. 35 (1), 53–80. http://dx.doi.org/10.1016/0079-6611(95)00005-2.

Belkin, I., 2004. Propagation of the "Great Salinity Anomaly" of the 1990s around the northern North Atlantic. Geophys. Res. Lett. 31. http://dx.doi.org/10.1029/2003GL019334.

Belkin, I.M., Levitus, S., Antonov, J., Malmberg, S.-A., 1998. "Great Salinity Anomalies" in the North Atlantic. Prog. Oceanogr. 41, 1–68.

Beszczynska-Möller, A., Woodgate, R.A., Lee, C., Melling, H., Karcher, M., 2011. A synthesis of exchanges through the main oceanic gateways to the Arctic Ocean. Oceanography 24, 82–89. http://dx.doi.org/10.5670/oceanog.2011.59.

Bhatt, U.S., et al., 2014. Implications of Arctic sea ice decline for the earth system. Annu. Rev. Environ. Resour. 39, 57–89.

Bintanja, R., Selten, F.M., 2014. Future increases in Arctic precipitation linked to local evaporation and sea-ice retreat. Nature 509, 479–482. http://dx.doi.org/10.1038/nature13259.

Björk, G., 1989. A one-dimensional time-dependent model for the vertical stratification of the upper Arctic Ocean. J. Phys. Oceanogr. 19, 52–67.

Carmack, E., 2007. The alpha/beta ocean distinction: a perspective on freshwater fluxes, convection, nutrients and productivity in high-latitude seas. Deep-Sea Res. II 54, 2578–2598.

Carmack, E., McLaughlin, F., 2011. Towards recognition of physical and geochemical change in Subarctic and Arctic seas. Prog. Oceanogr. 90, 90–104.

Comiso, J.C., 2012. Large decadal decline of the Arctic multiyear ice cover. J. Clim. 25. http://dx.doi.org/10.1175/JCLI-D-11-00113.1.

Condron, A., Winsor, P., Hill, C., Menemenlis, D., 2009. Simulated response of the Arctic freshwater budget to extreme NAO forcing. J. Clim. 22, 2422–2437. http://dx.doi.org/10.1175/2008JCLI2626.1.

Cullather, R.I., Bosilovich, M.G., 2011. The moisture budget of the polar atmosphere in MERRA. J. Clim. 24, 2861–2879. http://dx.doi.org/10.1175/2010JCLI4090.1.

Cuny, J., Rhines, P.B., Kwok, R., 2005. Davis Strait volume, freshwater, and heat fluxes. Deep-Sea Res. I 52, 519–542.

Curry, R.G., Mauritzen, C., 2005. Dilution of the northern North Atlantic Ocean in recent decades. Science 308, 1772–1774.

Curry, B., Lee, C.M., Petrie, B., Moritz, R.E., Kwok, R., 2014. Multi-year volume, freshwater, and heat transports through Davis Strait, 2004–2010. J. Phys. Oceanogr. 44, 1244–1266. http://dx.doi.org/10.1175/JPO-D-13-0177.1.

Day, C.G., 1968. Current measurements in Smith Sound, summer 1963. Tech. Rep. 16. U.S.C.G. Oceanogr. Rep.

de Steur, L., Hansen, E., Gerdes, R., Karcher, M., Fahrbach, E., Holfort, J., 2009. Freshwater fluxes in the East Greenland Current: a decade of observations. Geophys. Res. Lett. 36, L23,611. http://dx.doi.org/10.1029/2009GL041278.

de Steur, L., et al., 2013. Hydrographic changes in the Lincoln Sea in the Arctic Ocean with focus on an upper ocean freshwater anomaly between 2007–2010. J. Geophys. Res. http://dx.doi.org/10.1002/jgrc.20341.

de Steur, L., Hansen, E., Mauritzen, C., Beszczynska-Möller, A., Fahrbach, E., 2014. Impact of recirculation on the East Greenland Current in Fram Strait: results from moored current meter measurements between 1997 and 2009. Deep-Sea Res. I 92, 26–40. http://dx.doi.org/10.1029/2009GL041278.

Dee, D.P., et al., 2011. The ERA-Interim reanalysis: configuration and performance of the data assimilation system. Q. J. R. Meteorol. Soc. 137, 553–597. http://dx.doi.org/10.1002/qj.828.

Dickson, R.R., Meincke, J., Malmberg, S.-A., Lee, A.J., 1988. The "Great Salinity Anomaly" in the northern North Atlantic 1968–1982. Prog. Oceanogr. 20, 103–151.

Dickson, R.R., Osborn, T.J., Hurrell, J.W., Meincke, J., Blindheim, J., Adlandsvik, B., Vinje, T., Alekseev, G., Maslowski, W., 2000. The Arctic Ocean response to the North Atlantic Oscillation. J. Clim. 13, 2671–2696.

Dickson, R.R., Dye, S., Karcher, M., Meincke, J., Rudels, B., Yashayaev, I., 2007. Current estimates of freshwater flux through Arctic and subarctic seas. Prog. Oceanogr. 73, 210–230.

Dickson, B., et al., 2008. The overflow flux west of Iceland: variability, origins and forcing. In: Dickson, R.R., Meincke, J., Rhines, P. (Eds.), Arctic–Subarctic Ocean Fluxes: Defining the Role of the Northern Seas in Climate. Springer-Verlag, pp. 443–474.

Dmitrenko, I.A., Kirillov, S.A., Tremblay, L.B., 2008. The long-term and interannual variability of summer fresh water storage over the eastern Siberian shelf: implication for climatic change. J. Geophys. Res. 113. http://dx.doi.org/10.1029/2007JC004304.

Dodd, P.A., Heywood, K.J., Meredith, M.P., Naveira-Garabato, A.C., Marca, A.D., Falkner, K.K., 2009. Sources and fate of freshwater exported in the East Greenland Current. Geophys. Res. Lett. 36, L19608. http://dx.doi.org/10.1029/2009GL039663.

Dodd, P.A., Rabe, B., Hansen, E., Falck, E., Mackensen, A., Rohling, E., Stedmon, C., Kristiansen, S., 2012. The freshwater composition of the Fram Strait outflow derived from a decade of tracer measurements. J. Geophys. Res. 117, C11005. http://dx.doi.org/10.1029/2012JC008011.

Ekwurzel, B., Schlosser, P., Mortlock, R.A., Fairbanks, R.G., 2001. River runoff, sea ice meltwater, and Pacific water distribution and mean residence times in the Arctic Ocean. J. Geophys. Res. 106. http://dx.doi.org/10.1029/1999JC000024.

Falck, E., Kattner, G., Budéus, G., 2005. Disappearance of Pacific Water in the northwestern Fram Strait. Geophys. Res. Lett. http://dx.doi.org/10.1029/2005GL023400.

Fer, I., 2009. Weak vertical diffusion allows maintenance of cold halocline in the central Arctic. Atmos. Ocean. Sci. Lett. 2, 148–152.

Fowler, G.A., Siddall, G.R., Prinsenberg, S.J., 2004. An energy-conserving oceanographic profiler for use under mobile ice cover: ICYCLER. Int. J. Offshore Polar Eng. 14 (3), 176–181.

Fowler, C., Emery, W., Tschudi, M., 2013. Polar Pathfinder Daily 25 km EASE-Grid Sea Ice Motion Vectors. Version 2. Tech. Rep.National Snow and Ice Data Center, Boulder, Colorado, USA

Gelderloos, R., Straneo, F., Katsman, C.A., 2012. Mechanisms behind the temporary shutdown of deep convection in the Labrador Sea: lessons from the Great Salinity Anomaly years 1968–71. J. Clim. 25, 6743–6755. http://dx.doi.org/10.1175/JCLI-D-11-00549.1.

Giles, K.A., Laxon, S.W., Ridout, A.L., Wingham, D.J., Bacon, S., 2012. Western Arctic Ocean freshwater storage increased by wind-driven spin-up of the Beaufort Gyre. Nat. Geosci. http://dx.doi.org/10.1038/NGEO1379.

Hansen, E., Gerland, S., Granskog, M.A., Pavlova, O., Renner, A.H.H., Haapala, J., Løyning, T.B., Tschudi, M., 2013. Thinning of Arctic sea ice observed in Fram Strait: 1990–2011. J. Geophys. Res. 18, 5202–5221. http://dx.doi.org/10.1002/jgrc.20393.

Holland, M.M., Finnis, J., Barrett, A.P., Serreze, M.C., 2007. Projected changes in arctic ocean freshwater budgets. J. Geophys. Res. 112, G04S55. http://dx.doi.org/10.1029/2006JG000354.

Hunkins, K., Whitehead, J.A., 1992. Laboratory simulation of exchange through Fram Strait. J. Geophys. Res. 97, 11,299–11,321.

IPCC, 2007. Climate Change 2007: The Physical Science Basis. Contribution of Working Group I to the Fourth Assessment Report of the IPCC. In: Solomon, S., Qin, D., Manning, M., Chen, Z., Marquis, M., Averyt, K.B., Tignor, M., Miller, H.L. (Eds.), Cambridge University Press, Cambridge, United Kingdom and New York, NY, USA.

Jahn, A., Tremblay, L.B., Newton, R., Holland, M.M., Mysak, L.A., Dmitrenko, I.A., 2010. A tracer study of the Arctic Ocean's liquid freshwater export variability. J. Geophys. Res. 115, C07015. http://dx.doi.org/10.1029/2009JC005873.

Jahn, A., et al., 2012. Arctic Ocean freshwater: how robust are model simulations? J. Geophys. Res. 117, C00D16. http://dx.doi.org/10.1029/2012JC007907.

Jakobsson, M., et al., 2007. The early miocene onset of a ventilated circulation regime in the Arctic Ocean. Nature 447, 986–990. http://dx.doi.org/10.38/nature05924.

Jones, E.P., Anderson, L.G., Swift, J.H., 1998. Distribution of Atlantic and Pacific waters in the upper Arctic Ocean: implications for circulation. Geophys. Res. Lett. 25, 765–768.

Jones, E.P., Swift, J.H., Anderson, L.G., Lipizer, M., Civitarese, G., Falkner, K.K., Kattner, G., McLaughlin, F., 2003. Tracing Pacific water in the North Atlantic Ocean. J. Geophys. Res. 108. http://dx.doi.org/10.1029/2001JC001141.

Jones, E.P., Anderson, L.G., Jutterström, S., Swift, J.H., 2008. Sources and distribution of fresh water in the East Greenland Current. Prog. Oceanogr. 78, C00D16.

Kalnay, E., et al., 1996. The NCEP-NCAR 40-year reanalysis project. Bull. Am. Meteorol. Soc. 77, 437–471.

Karcher, M.J., Gerdes, R., Kauker, F., Köberle, C., Yashayaev, I., 2005. Arctic Ocean change heralds North Atlantic freshening. Geophys. Res. Lett. 32. http://dx.doi.org/10.1029/2005GL023861.

Kattsov, V.M., Walsh, J.E., Chapman, W.L., Govorkova, V.A., Pavlova, T.V., Zhang, X., 2007. Simulation and projection of Arctic freshwater budget components by the IPCC AR4 global climate models. J. Hydrometeorol. 8, 571–589. http://dx.doi.org/10.1175/JHM575.1.

Köberle, C., Gerdes, R., 2003. Mechanisms determining the variability of Arctic sea ice conditions and export. J. Clim. 16, 2843–2858.

Köberle, C., Gerdes, R., 2007. Simulated variability of the Arctic Ocean freshwater balance 1948–2001. J. Phys. Oceanogr. 37, 1628–1644.

Koenigh, T., Mikolajewicz, U., Haak, H., Jungclaus, J., 2007. Arctic freshwater export in the 20th and 21st centuries. J. Geophys. Res. 112, G04S41. http://dx.doi.org/10.1029/2006JG000274.

Kwok, R., 2009. Outflow of Arctic Ocean sea ice into the Greenland and Barents Seas: 1979–2007. J. Clim. 22, 2438–2457. http://dx.doi.org/10.1175/2008JCLI2819.1.

Kwok, R., Cunningham, G.F., 2010. Contribution of melt in the Beaufort Sea to the decline in Arctic multiyear sea ice coverage: 1993–2009. Geophys. Res. Lett. 37, L20501. http://dx.doi.org/10.1029/2010GL044678.

Kwok, R., Rothrock, D.A., 1999. Variability of Fram Strait ice flux and North Atlantic Oscillation. J. Geophys. Res. 104, 5177–5189.
Kwok, R., Rothrock, D.A., 2009. Decline in Arctic sea ice thickness from submarine and ICES at records: 1958–2008. Geophys. Res. Lett. 36, L15501. http://dx.doi.org/10.1029/2009GL039035.
Kwok, R., Cunningham, G.F., Pang, S.S., 2004. Fram Strait sea ice outflow. J. Geophys. Res. 109, C01009. http://dx.doi.org/10.1029/2003JC001785.
Kwok, R., Pedersen, L.T., Gudmandsen, P., Pang, S.S., 2007. Large sea ice outflow into the Nares Strait in 2007. Geophys. Res. Lett. 37, L03502. http://dx.doi.org/10.1029/2009GL041872.
Kwok, R., Cunningham, G.F., Wensnahan, M., Rigor, I., Zwally, H.J., Yi, D., 2009. Thinning and volume loss of the Arctic Ocean sea ice cover: 2003–2008. J. Geophys. Res. 114, C07005. http://dx.doi.org/10.1029/2009JC05312.
Kwok, R., Spreen, G., Pang, S., 2013. Arctic sea ice circulation and drift speed: decadal trends and ocean currents. J. Geophys. Res. 118. http://dx.doi.org/10.1002/jgrc.20191.
Laxon, S., Peacock, N., Smith, D., 2003. High interannual variability of sea ice thickness in the Arctic region. Nature 425, 947–950.
Laxon, S.W., et al., 2013. Cryosat-2 estimates of Arctic sea ice thickness and volume. Geophys. Res. Lett. 40, 732–737. http://dx.doi.org/10.1002/grl.50193.
Ledwell, J.R., Watson, A.J., Law, C.S., 1993. Evidence for slow mixing across the pycnocline from an open-ocean tracer-release experiment. Nature 364, 701–703.
Lewis, E.L., Jones, E.P., Lemke, P., Prowse, T.D., Wadhams, P. (Eds.), 2000. The Freshwater Budget of the Arctic Ocean vol. 70. Kluwer Academic Pub.
Lindsay, R., Wensnahan, M., Schweiger, A., Zhang, J., 2014. Evaluation of seven different atmospheric reanalysis products in the Arctic. J. Clim. 27, 2588–2606. http://dx.doi.org/10.1175/JCLI-D-13-00014.1.
Macdonald, R.W., Carmack, E.C., McLaughlin, F.A., Falkner, K.K., Swift, J.H., 2012. Connections among ice, runoff and atmospheric forcing in the Beaufort Gyre. Geophys. Res. Lett. 26 (15), 2223–2226. http://dx.doi.org/10.1029/1999GL900508.
Mauritzen, C., 2012. Arctic freshwater. Nat. Geosci. 5, 162–164.
McGeehan, T., Maslowski, W., 2012. Evaluation and control mechanisms of volume and freshwater export through the Canadian Arctic Archipelago in a high-resolution pan-Arctic ice-ocean model. J. Geophys. Res. 117, C00D14. http://dx.doi.org/10.1029/2011JC007261.
McLaughlin, F.A., Carmack, E.C., Macdonald, R.W., Bishop, J.K.B., 1996. Physical and geochemical properties across the Atlantic/Pacific water mass front in the southern Canadian Basin. J. Geophys. Res. 101, 1183–1197. http://dx.doi.org/10.1029/95JC02634.
McPhee, M.G., Proshutinsky, A., Morison, J.H., Steele, M., Alkire, M.B., 2009. Rapid change in freshwater content of the Arctic Ocean. J. Geophys. Res. 36. http://dx.doi.org/10.1029/2009GL037525.
Melling, H., et al., 2008. Fresh-water fluxes via Pacific and Arctic outflows across the Canadian polar shelf. In: Dickson, R.R., Meincke, J., Rhines, P. (Eds.), Arctic–Subarctic Ocean Fluxes: Defining the Role of the Northern Seas in Climate. Springer-Verlag, pp. 193–247.
Melling, H., 2011. The best laid schemes: a Nares Strait adventure. Oceanography 24 (3), 124–125. http://dx.doi.org/10.5670/oceanog.2011.63.
Morison, J., Kwok, R., Peralta-Ferriz, C., Alkire, M., Rigor, I., Andersen, R., Steele, M., 2012. Changing Arctic Ocean freshwater pathways. Nature 481. http://dx.doi.org/10.1038/nature10705.
Münchow, A., Melling, H., 2008. Ocean current observations from Nares Strait to the west of Greenland: interannual to tidal variability and forcing. J. Mar. Res. 66, 801–833.
Münchow, A., Melling, H., Falkner, K.K., 2006. An observational estimate of volume and freshwater flux leaving the Arctic Ocean through Nares Strait. J. Phys. Oceanogr. 36, 2025–2041.
Münchow, A., Falkner, K.K., Melling, H., 2007. Spatial continuity of measured seawater and tracer fluxes through Nares Strait, a dynamically wide channel bordering the Canadian Archipelago. J. Mar. Res. 65, 759–788.
Newton, R., Schlosser, P., Mortlock, R., Swift, J., MacDonald, R., 2013. Canadian basin freshwater sources and changes: results from the 2005 Arctic Ocean section. J. Geophys. Res. 118 (4), 2133–2154. http://dx.doi.org/10.1002/jgrc.20101.
Nghiem, S.V., Rigor, I.G., Perovich, P.C.-C.D.K., Weatherly, J.W., Neumann, G., 2007. Rapid reduction of Arctic perennial sea ice. Geophys. Res. Lett. 34, L19504. http://dx.doi.org/10.1029/2007GL031138.
Nilsson, J., Walin, G., 2010. Salinity-dominated thermohaline circulation in sill basins: can two stable equilibria exist? Tellus 62 (2), 123–133.
Notz, D., Marotzke, J., 2012. Observations reveal external driver for Arctic sea-ice retreat. Geophys. Res. Lett. 39. http://dx.doi.org/10.1029/2012GL051094.
Ogi, M., Yamazaki, K., Tachibana, Y., 2004. The summertime annular mode in the northern hemisphere and its linkage to the winter mode. J. Geophys. Res. 109. http://dx.doi.org/10.1029/2004JD004514.
Peterson, B.J., McClelland, J., Curry, R., Holmes, R.M., Walsh, J.E., Aagaard, K., 2006. Trajectory shifts in the Arctic and subarctic freshwater cycle. Science 313, 1061–1066.
Peterson, I., Hamilton, J., Prinsenberg, S.J., Pettipas, R., 2012. Wind-forcing of volume transport through Lancaster Sound. J. Geophys. Res. 117, C11,018. http://dx.doi.org/10.1029/2012JC008140.
Prinsenberg, S.J., Hamilton, J., 2005. Monitoring the volume, freshwater and heat fluxes passing through Lancaster Sound in the Canadian Arctic Archipelago. Atmosphere–Ocean 43 (1), 1–22.
Prinsenberg, S., Hamilton, J., Peterson, I., Pettipas, R., 2009. Observing and interpreting the seasonal variability of the oceanographic fluxes passing through Lancaster Sound of the Canadian Arctic Archipelago. In: Nihoul, J., Kostianoy, A. (Eds.), Influence of Climate Change on the Changing Arctic and Sub-Arctic Conditions. Springer, pp. 549–587.
Proshutinsky, A.Y., Johnson, M.A., 1997. Two circulation regimes of the wind-driven Arctic Ocean. J. Geophys. Res. 102, 12,493–12,514.
Proshutinsky, A., et al., 2009. Beaufort Gyre freshwater reservoir: state and variability from observations. J. Geophys. Res. 114. http://dx.doi.org/10.1029/2008JC005104.
Proshutinsky, A., et al., 2011. Recent advances in Arctic Ocean studies employing models from the Arctic Ocean Model Intercomparison Project. Oceanography 24. http://dx.doi.org/10.5670/oceanog.2011.61.
Rabe, B., Karcher, M., Schauer, U., Toole, J.M., Krishfield, R.A., Pisarev, S., Kauker, F., Gerdes, R., Kikuchi, T., 2011. An assessment of Arctic Ocean freshwater content changes from the 1990s to the 2006–2008 period. Deep-Sea Res. I 58, 173–185. http://dx.doi.org/10.1016/j.dsr.2010.12.002.
Rabe, B., Johnson, H.L., Münchow, A., Melling, H., 2012. Geostrophic ocean currents and freshwater fluxes across the Canadian Polar Shelf via Nares Strait. J. Mar. Res. 70, 603–640.
Rabe, B., et al., 2013. Liquid export of Arctic freshwater components through the Fram Strait 1998–2011. Ocean Sci. 9, 91–109. http://dx.doi.org/10.5194/osd-9-91-2013.
Rabe, B., Karcher, M., Kauker, F., Schauer, U., Toole, J.M., Krishfield, R.A., Pisarev, S., Kikuchi, T., Su, J., 2014. Arctic Ocean basin liquid freshwater storage trend 1992–2012. Geophys. Res. Lett. 41, 961–968. http://dx.doi.org/10.1002/2013GL058121.
Rawlins, M.A., et al., 2010. Analysis of the Arctic system for freshwater cycle intensification: observations and expectations. J. Clim. 21, 5715–5737. http://dx.doi.org/10.1175/2010JCLI3421.1.
Rigor, I.G., Wallace, J.M., 2004. Variations in the age of Arctic sea-ice and summer sea-ice extent. Geophys. Res. Lett. 31, L09401. http://dx.doi.org/10.1029/2004GL019492.
Rigor, I.G., Wallace, J.M., Colony, R.L., 2002. Response of sea ice to the Arctic Oscillation. J. Clim. 15, 2,648–2,663.
Rothrock, D.A., Yu, Y., Maykut, G.A., 1999. Thinning of the Arctic sea-ice cover. Geophys. Res. Lett. 26, 3469–3472.
Rudels, B., 1986. The outflow of polar water through the Arctic Archipelago and the oceanographic conditions in Baffin Bay. Polar Res. 4, 161–180. http://dx.doi.org/10.1111/j.1751-8369.1986.tb00528.x.
Rudels, B., 1989. The formation of Polar Surface Water, the ice export and the exchanges through the Fram Strait. Prog. Oceanogr. 22, 205–248.
Rudels, B., 2010. Constraints on exchanges in the Arctic Mediterranean—do they exist and can they be of use? Tellus 62A, 109–122. http://dx.doi.org/10.1111/j/1600-0870.2009.00425.x.
Rudels, B., 2011. Volume and freshwater transports through the Canadian Arctic Archipelago–Baffin Bay system. J. Geophys. Res. 116. http://dx.doi.org/10.1029/2011JC007019.
Rudels, B., Friedrich, H.J., 2000. The transformations of Atlantic Water in the Arctic Ocean and their significance for the freshwater budget. In: Lewis, E.L., Jones, P.E., Lemke, P., Prowse, T.D., Wadhams, P. (Eds.), The Freshwater Budget of the Arctic Ocean. NATO Science Series vol. 70. Springer, Netherlands, pp. 503–532. http://dx.doi.org/10.1007/978-94-011-4132-1_21.
Rudels, B., Anderson, L.G., Jones, E.P., 1996. Formation and evolution of the surface mixed layer and halocline of the Arctic Ocean. J. Geophys. Res. 101, 8807–8821.
Rudels, B., Jones, E.P., Schauer, U., Eriksson, P., 2004. Atlantic sources of the Arctic Ocean surface and halocline waters. Polar Res. 23, 181–208.
Rudolf, B., Becker, A., Schneider, U., Meyer-Christoffer, A., Ziese, M., 2010. GPCC Status Report December 2010. Tech. Rep.Global Precipitation Climatology Centre (GPCC)
Sadler, H.E., 1976. Water, heat and salt transports through Nares Strait, Ellesmere Island. J. Fish. Res. Board Can. 33 (10), 2286–2295.
Samleson, R.M., Agnew, T., Melling, H., Münchow, A., 2006. Evidence for atmospheric control of sea-ice motion through Nares Strait. Geophys. Res. Lett. 33, L02506. http://dx.doi.org/10.1029/2005GL025016.
Schlosser, P., Bauch, D., Fairbanks, R., Bönisch, G., 1994. Arctic river run-off: mean residence time on the shelves and in the halocline. Deep-Sea Res. I 41 (7), 1053–1068.
Schlosser, P., Bönisch, G., Kromer, B., Loosli, H., Bühler, R., Bayer, R., Bonani, G., Koltermann, K.P., 1995. Mid-1980s distribution of tritium, ^{3}He, ^{14}C and ^{39}Ar in the Greenland/Norwegian Seas and the Nansen Basin of the Arctic Ocean. Prog. Oceanogr. 35 (1), 1–28. http://dx.doi.org/10.1016/0079-6611(95)00003-Y.
Schmitt, R.W., Bogden, P.S., Dorman, C.E., 1989. Evaporation minus precipitation and density fluxes for the North Atlantic. J. Phys. Oceanogr. 19, 1208–1221.
Serreze, M.C., Barrett, A.P., 2011. Characteristics of the Beaufort Sea High. J. Clim. 24. http://dx.doi.org/10.1175/2010JCLI3636.1.
Serreze, M.C., et al., 2006. The large-scale freshwater cycle of the Arctic. J. Geophys. Res. 111, C11010. http://dx.doi.org/10.1029/2005JC003424.
Serreze, M.C., Barrett, A.P., Slater, A.G., 2008. Variability and change in the atmospheric branch of the Arctic hydrological cycle. In: Dickson, R.R., Meincke, J., Rhines, P. (Eds.), Arctic–Subarctic Ocean Fluxes: Defining the Role of the Northern Seas in Climate. Springer-Verlag, pp. 343–362.
Shiklomanov, A., 2010. River discharge. In: Richter-Menge, J., Overland, J.E. (Eds.), Arctic Report Card 2010. NOAA, pp. 38–40.
Shiklomanov, I.A., Shiklomanov, A.I., Lammers, R.B., Peterson, B.J., Vorosmarty, C.J., 2000. The dynamics of river water inflow to the Arctic Ocean. In: Lewis, E.L., Jones, E.P., Lemke, P., Prowse, T.D., Wadhams, P. (Eds.), The Freshwater Budget of the Arctic Ocean. Kluwer Academic Publishers, Dordrecht/Boston/London, pp. 281–296.
Spreen, G., Kern, S., Stammer, D., Hansen, E., 2009. Fram Strait sea ice volume export estimated between 2003 and 2008 from satellite data. Geophys. Res. Lett. 36, L19,502. http://dx.doi.org/10.1029/2009GL039591.
Steele, M., Boyd, T., 1998. Retreat of the cold halocline layer in the Arctic Ocean. J. Geophys. Res. 103, 10,419–10,435.
Steele, M., Ermold, W., 2004. Salinity trends on the Siberian shelves. Geophys. Res. Lett. 31, L24308. http://dx.doi.org/10.1029/2004GL021302.
Steele, M., Morley, R., Ermold, W., 2001. A global ocean hydrography with a high quality Arctic Ocean. J. Clim. 14, 2079–2087.
Steele, M., Morison, J., Ermold, W., Rigor, I., Ortmeyer, M., 2004. Circulation of summer Pacific halocline water in the Arctic Ocean. J. Geophys. Res. 109, C02027. http://dx.doi.org/10.1029/2003JC002009.
Stewart, K.D., Haine, T.W.N., 2013. Wind-driven Arctic freshwater anomalies. Geophys. Res. Lett. 40. http://dx.doi.org/10.1002/2013GL058247.

Stigebrandt, A., 1981. A model for the thickness and salinity of the upper layers of the arctic ocean and the relation between the ice thickness and some external parameters. J. Phys. Oceanogr. 11, 1407–1422.
Stigebrandt, A., 1984. The North Pacific: a global-scale estuary. J. Phys. Oceanogr. 14, 464–470.
Straneo, F., Saucier, F.J., 2008. The Arctic–subarctic exchange through Hudson Strait. In: Dickson, R.R., Meincke, J., Rhines, P. (Eds.), Arctic–Subarctic Ocean Fluxes: Defining the Role of the Northern Seas in Climate. Springer-Verlag, pp. 249–261.
Sundby, S., Drinkwater, K., 2007. On the mechanisms behind salinity anomaly signals of the northern North Atlantic. Prog. Oceanogr. 73, 190–202.
Swift, J.H., Aagaard, K., Timokhov, L., Nikiforov, E.G., 2005. Long-term variability of Arctic Ocean waters: evidence from a reanalysis of the EWG data set. J. Geophys. Res. 110, C03012. http://dx.doi.org/10.1029/2004JC002312.
Taylor, J.R., Falkner, K.K., Schauer, U., Meredith, M., 2003. Quantitative considerations of dissolved barium as a tracer in the Arctic Ocean. J. Geophys. Res. 108. http://dx.doi.org/10.1029/2002JC001635.
Terrainbase, 1995. TerrainBase, Global 5 arc-minute ocean depth and land elevation from the US National Geophysical Data Center. Tech. Rep.NGDC/NESDIS/NOAA/US Department of Commerce Research Data Archive at the NCAR Computational and Information Systems Laboratory (accessed 22Jan2013)
Thompson, D.W.J., Wallace, J.M., 1998. The Arctic Oscillation signature in the wintertime geopotential height and temperature fields. Geophys. Res. Lett. 25, 1297–1300.
Travers, C., 2012. Quantifying Sea-ice Volume Flux Using Moored Instrumentation in the Bering Strait. (Master's thesis). University of Washington.
Tsubouchi, T., et al., 2012. The Arctic Ocean in summer: a quasi-synoptic inverse estimate of boundary fluxes and water mass transformation. J. Geophys. Res. 117, C01,024. http://dx.doi.org/10.1029/2011JC007174.
Uppala, S.M., et al., 2005. The ERA-40 re-analysis. Q. J. R. Meteorol. Soc. 131 (612), 2961–3012. http://dx.doi.org/10.1256/qj.04.176.
Vaughan, D.G., et al., 2013. Observations: cryosphere. In: Stocker, T.F., Qin, D., Plattner, G.-K., Tignor, M., Allen, S.K., Boschung, J., Nauels, A., Xia, Y., Bex, V., Midgley, P. (Eds.), Climate Change 2013: The Physical Science Basis. Contribution of Working Group I to the Fifth Assessment Report of the Intergovernmental Panel on Climate Change. Cambridge University Press, Cambridge, United Kingdom and New York, NY, USA.
Vavrus, S.J., Holland, M.M., Jahn, A., Bailey, D., Blazey, B.A., 2012. Twenty-first-century Arctic climate change in CCSM4. J. Clim. 25, 2696–2710.
Vinje, T., 2001. Fram Strait ice fluxes and the atmospheric circulation: 1950–2000. J. Clim. 14, 3508–3517.
Vinje, T., Nordlund, N., Kvambekk, A., 1998. Monitoring ice thickness through Fram Strait. J. Geophys. Res. 104, 10,437–10,449.
Wadhams, P., Gill, A., Linden, P.F., 1979. Transect by submarine of the East Greenland Front. Deep-Sea Res. A 26, 1311–1327.
Wadley, M.R., Bigg, G.R., 2004. "Great Salinity Anomalies" in a coupled climate model. Geophys. Res. Lett. 31. http://dx.doi.org/10.1029/2004GL020426.
Wadley, M.R., Bigg, G.R., 2006. Are "Great Salinity Anomalies" advective? J. Climate Spec. Sect. 19, 1080–1087.
Webster, S., Lee, C., Gobat, J., 2014. Preliminary results in under-ice acoustic navigation for seagliders in Davis Strait. Oceans '14 MTS/IEEE Conference, St. John's, Newfoundland, Canada, vol. to appear.
Werenskiold, W., 1935. Coastal currents. Geophys. Publ. 10 (13) (14 pp.).
White, D., et al., 2007. The Arctic freshwater system: changes and impacts. J. Geophys. Res. 112 (G4), G04S54. http://dx.doi.org/10.1029/2006JG000353.
Woodgate, R.A., Aagaard, K., 2005. Revising the Bering Strait freshwater flux into the Arctic Ocean. Geophys. Res. Lett. 32. http://dx.doi.org/10.1029/2004GL021747.
Woodgate, R.A., Aagaard, K., Weingartner, T.J., 2005. A year in the physical oceanography of the Chukchi Sea: moored measurements from autumn 1990–1991. Deep-Sea Res. II 52 (24–26), 3116–3149.
Woodgate, R.A., Aagaard, K., Weingartner, T.J., 2006. Interannual changes in the Bering Strait fluxes of volume, heat and freshwater between 1991 and 2004. Geophys. Res. Lett. 33, L15609. http://dx.doi.org/10.1029/2006GL026931.
Woodgate, R.A., Weingartner, T.J., Lindsay, R., 2012. Observed increases in Bering Strait oceanic fluxes from the Pacific to the Arctic from 2001 to 2011 and their impacts on the Arctic Ocean water column. Geophys. Res. Lett. 39, L24603. http://dx.doi.org/10.1029/2012GL054092.
Yamamoto-Kawai, M., McLaughlin, F.A., Carmack, E.C., Nishino, S., Shimada, K., Kurita, N., 2009. Surface freshening of the Canada Basin, 2003–2007: river runoff versus sea ice meltwater. J. Geophys. Res. 114, C00A05. http://dx.doi.org/10.1029/2008JC005000.
Zhang, J., Rothrock, D.A., 2003. Modeling global sea ice with a thickness and enthalpy distribution model in generalized curvilinear coordinates. Mon. Weather Rev. 131, 845–861.